Generic integration tools for reconfigurable laser micromachining systems

Dimov, Stefan; Penchev, Pavel; Bhaduri, Debajyoti; Soo, Sein

DOI:
10.1016/j.jmsy.2015.10.006

Document Version
Peer reviewed version

Citation for published version (Harvard):
Dimov, S, Penchev, P, Bhaduri, D & Soo, S 2016, 'Generic integration tools for reconfigurable laser micromachining systems', *Journal of Manufacturing Systems*, vol. 38, pp. 27-45.
https://doi.org/10.1016/j.jmsy.2015.10.006

Accepted Manuscript in Journal of Manufacturing Systems on 01/11/2015

Generic integration tools for reconfigurable laser micromachining systems

Pavel Penchev[1], Stefan Dimov[1], Debajyoti Bhaduri[1] and Sein L Soo[1]
[1] (School of Mechanical Engineering), University of Birmingham, UK
Corresponding Author:
Pavel Penchev, School of Mechanical Engineering, University of Birmingham, Edgbaston, Birmingham B15 2TT, UK
Email:pxp931@bham.ac.uk

Abstract

Laser micro-machining (LMM) is an attractive manufacturing process due to its intrinsic machining characteristics such as such as non-contact processing and capabilities to machine complex free-form surfaces in a wide range of materials. Nevertheless, state-of- art LMM platforms still do not offer the repeatability, reproducibility and operability of conventional machining centres, e.g. the flexibility to realise complex machining configurations and also to combine LMM with other complementary processes in hybrid manufacturing systems and production lines. The paper presents the development of three generic integration tools for improving the system-level performance of reconfigurable LMM platforms. In particular, the research reports the design and implementation of modular workpiece holding device, automated workpiece setting up routine and automated strategy for multi-axis LMM machining employing rotary stages. An experimental validation of their accuracy, repeatability and reproducibility (ARR) are performed on a representative state-of-art LMM platform. The results demonstrate the flexibility and operability of the proposed tools to address important system-level issues in LMM by creating the necessary pre-requisites for achieving machining ARR better than +/- 10 μm.

Keywords: laser micro-machining; reconfigurable machine tools; modular workpiece holding devices; multi-axis machining strategy; automated workpiece setting-up routines.

1. Introduction

Technological advances across different application areas, e.g. micro-electromechanical systems, micro-sensor systems, microelectronics, smart communication systems and biomedical devices, have driven the demand for product miniaturization, increased accuracy and precision of products

while satisfying constantly growing requirements for production efficiency and reliability and improved environmental footprint [1 - 3]. To address both product and process development requirements underpinning the product miniaturisation trends, considerable research efforts are focused on increasing the capabilities of various manufacturing processes such as milling, forming, additive manufacturing and laser processing. Also, this includes the development of hybrid manufacturing platforms that combine innovatively the capabilities of complimentary processes and thus to exploit the advantages offered by their integrations while overcoming some of their shortcomings [1].

Laser micro-machining (LMM) is a research and development area that have been attracting a significant interest both from the research community and industry due to its appealing intrinsic machining characteristics such as non-contact processing, capabilities to machine complex free-form (3D) surfaces in a wide range of materials and also to combine/integrate with other complementary processes in manufacturing platforms. Other important reasons are the underlining advances in laser technology to meet manufacturing requirements for increased throughput and quality of miniaturised products that incorporate functional features with different scales and geometrical complexity while extending the process capabilities for in-situ selective surface treatment and functionalization [4-6]. Some examples that demonstrate the wide ranging manufacturing capabilities of the LMM technology in different industrial sectors and contexts are the production of: aspheric micro-lens on transparent materials [7], coronary stents on metallic samples [8], MEMS-based variable capacitor device [9], a diffractive optical device on carbon nanotubes-based buckypaper [9] and replication masters with micro- and nano-scale features on bulk metallic glasses [11]. Furthermore, another direction in broadening the capabilities of the laser micro machining technology is its integration in hybrid manufacturing platforms [12]. For example, an integration of micro-milling and laser structuring was reported to produce complex biotechnology products with feature sizes smaller than the cutting tool diameter without compromising machining time [13].

However, the literature review reveals that even though commercial LMM platforms are available, the broader take up of this attractive manufacturing technology both as a stand-alone fabrication route and also as a component in hybrid manufacturing solutions is still to come [14]. A detailed capability maturity model of the process also shows that in comparison to micro-milling, which is ranked as a mature process and is widely used across different industrial sectors, laser micro processing is considered not sufficiently mature due to various open issues related to the process fundamental characteristics, process predictability and process reliability [15]. In addition, the literature shows that in the last two decades the research efforts were mainly focussed on investigating laser-material interactions, process modelling and empirical process optimization to address specific manufacturing requirements, such as surface integrity and processing time, while not paying sufficient attention to the development of generic tools and techniques for extending the LMM capabilities both as standalone machine tools or a component technology in manufacturing platforms. The research on improving the performance and reliability of LMM platforms as machine tools was mostly limited to:

- advances in optical beam deflection systems and their simultaneous use with mechanical stages for processing laser surface areas [16, 17];
- development of generic tools for counteracting the dynamics effects of optical beam delivery systems [18-20];
- Beam-path generation tools based on commercially available CAD/CAM systems for creating NC part programmes for machining components with high geometrical complexity [21 - 23].

At the same time there are significant advances in LMM component technologies, e.g. the growing number of short and ultrashort laser sources with constantly increasing maximum pulse energies and repetition rates [24], decreasing pulse durations and shorter wavelengths [25], ultra-high speed variable focus elements for advance beam delivery [26], high dynamics optical beam deflection systems with integrated digital scanner motor control electronics [27], linear and rotary mechanical axes with a repeatable positioning resolution of less than 0.1 µm and less than 30 µrad, respectively

[28]. Nevertheless, the advances in these component technologies do not immediately translate into improvements of the LMM performance at the system level in terms of machining accuracy, repeatability and reproducibility (ARR) unless adequate integration tools and techniques are used to achieve the necessary level of components' synergy without compromising their performance. The importance of integration tools and techniques in LMM installations is exemplified in a comparative study of three different LMM systems that have comparable component technologies with very similar specifications, but in spite of this, their ARR results were significantly different and far away from the stated specifications of the equipment manufacturers [29]. Thus, this reiterates the importance of developing and validating critical integration tools and techniques for LMM platforms and thus to bring the technology to a maturity level of well-established manufacturing processes such as micro-milling. Such research and development efforts are necessary to underpin both the standalone use of LMM systems and also their integration in hybrid manufacturing platforms in different application contexts.

This paper reports research on developing and validating generic system-level solutions for integrating component technologies in LMM and thus to improve significantly the process ARR. First, key component technologies of LMM systems are introduced and important integration solutions are identified by conducting a system-level critical analysis of state-of-the-art LMM platforms. Then, three generic integration tools are proposed and validated on a representative LMM system. Finally, conclusions are made about the capabilities of proposed system-level integration solutions.

2. System-level critical analysis of factors affecting the LMM performance

2.1 Component technologies' requirements

A reconfigurable LMM platform should have sufficient flexibility to realise different processing operations, e.g. structuring of parts that incorporate functional features with varying sizes and geometrical complexity, polishing of free-form parts, capability to process different materials, e.g. metals, polymers and glasses, while satisfying specific requirements in regards to ARR, surface

integrity and processing efficiency. Such concentration of operations in a single machining setup requires system-level functionalities that are determined both by the component technologies employed for their realisation and also by a range of integration tools and techniques used to assure their functional operability within predefined ARR constraints.

A system-level analysis of five different implementations of such reconfigurable LMM platforms was conducted to identify the common component technologies that were necessary for their implementation. It is important to note that the five investigated LLM systems integrate similar and in some case identical state-of-art representative component technologies and they are built by different system integrators. In this way an attempt was made to identify and assess objectively the system-level integration issues in implementing LMM systems. An example of such representative LLM platform is described in [51], while another representative laser micro-machining platform is presented and explained in details in Section 4.1. The results of this analysis are provided in Table 1, where their component technologies are split into two categories, in particular main component technologies, which were available across all LMM configurations and auxiliary ones, whose implementation and functionality varied between the platforms but were required to fulfil common requirements in regards to systems' operability, stability, flexibility and safety.

Table 1. Functional specification of component technologies for LMM

Main Component Technologies
• Short/ultra-short pulsed laser source(s) with capabilities to vary the average power, repetition rates, wavelengths and laser spot characteristics for realising different material processing mechanism
• 3D optical beam deflection system with high dynamics
• Focusing telecentric lens for a consistent beam incident angles within the field of view
• Linear mechanical stages with high positioning accuracy and precision to realise Infinite Field of View (IFV) processing
• Rotary mechanical stages for realizing different manufacturing configurations
• Measurement probes for inline inspection and alignment of parts
• Optical beam delivery path with capabilities to vary the beam spatial profile
Auxiliary Component Technologies
• Machine frame structure to minimise any disturbances from the surrounding environment
• Enclosure for Class 1 laser processing [30]
• Laser fume extractor
• Inline energy/power measurement device

• Laser beam profiler for setting up optimal laser machining parameters
• Modular workpiece holding for realising different machining configurations and robust integration into hybrid manufacturing systems
• Workpiece's setting up routines
• PC-based control system with specialised Graphical User Interface (GUI)

2.2 System-level integration issues

To conduct a critical analysis of integration issues in designing and implementing LMM platforms, it is very important to study laser systems with almost identical or comparable hardware configurations. Thus, any discrepancy in their LMM capabilities can be attributed mostly to system-level integration issues associated with their component technologies and to much lesser extend to their technical specifications. Therefore, three state-of-the-art LMM systems were selected to carry out this critical analysis. Key capabilities expected and also representative of those already available in reconfigurable LMM platforms were analysed. In particular, a comparative study to quantify the machining ARR of the three systems was conducted to identify significant discrepancies in their LMM capabilities [31]. The key capabilities considered are provided in Table 2 together with the results of the analysis of the three platforms that are denoted as A, B and C in Table 2.

Table 2. System-level capabilities of the three reconfigurable LMM platforms

1) Flexible workholding solutions for realising different machining configurations, i.e. for laser processing of axis-symmetric parts and multi-sides laser machining, and for seamless integration of LMM into hybrid manufacturing platforms	
System	Description
A	Custom-made workholding devices for positioning parts (individual solutions for different machining configurations/operations). No integration of LMM into a hybrid manufacturing system is envisaged.
B	In-house workholding devices are produced to meet different application requirements.
C	No special workholding devices. Mechanical stages are used to place samples in the laser system.
2) Automated routines/strategies for executing complex machining operations that require the utilization of both linear and rotary mechanical axes	
A	Not available and a custom-made solution under development.
B	Manual methods to utilize rotary and linear stages simultaneously.
C	No automated strategies are available.
3) Workpiece's setting up routines with pre-defined ARR	
A	Manual alignment employing a high resolution optical camera. Accuracy and repeatability better than 50 μm.
B	Alignment solution employing a confocal probe. Accuracy and repeatability better than

	20 µm.
C	Optical camera for lateral alignment and a confocal probe for setting up the machining surface. Accuracy and repeatability within +/-10 µm.
4) Control system with specialised LMM GUI	
A	A system/tool with specialised GUI realised in commercially available CAD software for entering different laser machining parameters and also for handling different input file formats.
B	A system with GUI for controlling laser machining parameters.
C	Several GUIs for different component technologies that run simultaneously to control laser machining parameters.
5) ARR achievable in different LMM operations	
A	ARR better than +/- 150 µm.
B	Accuracy within +/- 60 µm while repeatability and reproducibility are better than 20 µm.
C	ARR better than +/- 10 µm.

There are some other commercially available laser machining systems [32-34] that are designed for specific applications, in particular for producing cooling holes on aerospace components or structuring/texturing free-form surfaces of moulding tools. They are based on conventional machine tool platforms and thus their frame structures, PC-based control systems and workpiece setting up routines and equipment are the same as those used in multi-axis machining centres. Such system cannot be considered LMM platforms as they are standalone system designed for handling relatively big components, e.g. turbine blades and mould tools, while the laser machining system that are the focus of this research are for machining relatively small components, e.g. usually fitting within a working envelop of mm 65 x 65 mm x 10 mm and weight less than 1 kg. Therefore, they were not considered in the system-level analysis carried out in this research.

It is apparent from the system level analysis in Table 2 that even though all three LMM systems can provide extensive manufacturing capabilities, their available tools are not generic and far from what should be expected in machine tools for realising complex machining operations. Furthermore, the results of the comparative study also revealed substantial discrepancies in terms of ARR capabilities of the analysed three systems [31]. For example, the performance of System C was assessed to deliver ARR capabilities better than +/- 10 µm, while System A and B had ARR of +/- 150 µm and +/- 60 µm, respectively. Since, the hardware configurations of the three systems are comparable, the

discrepancies in terms of LMM systems performance clearly demonstrate the existence of system-level integration issues. In particular, the system-level issues that were identified as critical for improving the reliability, robustness and interoperability of LMM platforms and also to achieve the necessary machining ARR for their broader use are: the development of modular workpiece holding device, automated workpiece setting up routines and automated multi-axis machining strategies. The importance of these system-level integration solutions for achieving ARR that are commonly required across different application areas is further reinforced by the work reported by other researchers. In particular, in a study reporting the application of LMM for producing a ceramic microsurgical tool with features on two opposite sides of the component, a sequence of manual operations (fixing, repositioning and alignment in a single machining setup) were performed to manufacture the tool [35]. The system-level issues in this machine-fixture-component configuration had detrimental effects on the overall machining results, i.e accuracy of produced components was within +/- 70 μm while reproducibility was less 100 μm. Even though, the reported machining errors of the produced components were not critical for the parts' functionality, this case study points at some typical requirements that modular workpiece holding devices and automated workpiece setting up routines should fulfil to deliver higher ARR. In another case study on LMM of rollers, a rotary stage is used in a LMM platform [36]. It is stated that new software solutions were developed to achieve the required ARR in the used LMM configuration. Especially, these tools made possible the use of the rotary stages but they were only applicable for the processing of axis-symmetric parts, where the laser beam is fixed and thus the high dynamics of optical beam deflectors could not be used [36]. Again, this case study demonstrates how system-level limitations on the simultaneous use of optical and mechanical beam movements affect the capabilities of the LMM platforms, especially where high ARR are required.

3. Developments of system-level integration tools and techniques for LMM

3.1 Design and implementation of modular workpiece holding device

Based on the analysis of LMM industrial applications, where features with dimensions of less than 100 µm and accuracy better than 10 µm are required [37], the following generic considerations were identified that were taken into account when designing modular workpiece holding devices:

- High ARR achievable in positioning parts in LMM platforms;
- a modular design for realising different LMM configurations;
- designs based on standardized components for cost effective and robust implementation in different LMM configurations;
- compactness and minimal weight to minimise the negative dynamics effects on machining results;
- the necessity for common unifying solutions for integrating different modular technologies, e.g. machining, material processing, inspection and alignment, in hybrid manufacturing platforms;
- interchangeability for realising different LMM configurations and also to support both manual and automated workpiece setting up routines;

The workpiece holding device that was designed is schematically presented in Figure 1. It consists of standardized commercially available components that are well proven in different machining applications and at the same time do not require frequent maintenance [38]. In particular, the workpiece holding device consists of main and secondary assembly units. The main assembly unit incorporates a “macro” receiver that can be precisely fixed and referenced either to a mechanical stage (rotary or linear) or to any other surface of the machine frame structure and a drawbar that provides means to attach precisely various workpiece holding adapters/extensions to the receiver. The secondary assembly unit incorporates workpiece holding extensions that can ensure the necessary flexibility to meet the requirements for various laser machining operations. As shown in Figure 1, examples of workpiece holding extensions include:

- pallets - interface plate assemblies for holding prismatic parts in machining operations requiring only linear movements of mechanical stages,
- L-shaped brackets assembly for holding prismatic parts in machining operations requiring both linear and rotary movements of mechanical stages;
- chucks for holding axis-symmetric parts.

Thus, the modular design of the proposed workpiece holding device provide the flexibility and the robustness necessary to realize various LMM configurations . Figure 2 shows examples of manufacturing configurations that were implemented to test the proposed design. In particular, workpiece holding devices to carry out one-side processing of a single part or an array of parts, multi-side machining of parts, and processing of axis-symmetric parts. Since the different manufacturing extensions are accurately referenced via a system of datum points in the macro receiver and the pallet by applying a consistent force through the drawbar, different extensions can be easily integrated into the LMM platforms without the need for any manual setting up operations. This leads both to significant reduction in setting up time and also reduces uncertainty associated with workpieces' positioning in LMM platforms**.** Figure 1 also provides details about the masses of both the main assembly unit and also of each of the proposed workpiece holding extensions. Taking into account the capabilities of mechanical stages [39] and stacks of them in LMM platforms it can be concluded that the proposed workpiece holding device with a mass not exceeding 3.5 kg will have minimal negative dynamics effects on LMM operations. The modular design will also facilitate the integration of LMM operations in hybrid manufacturing systems. In particular, an installation of the main assembly units in each of the integrated processing steps in a hybrid manufacturing system allows workpieces to be mounted on a common holding extension and subsequently to be carried throughout all processing and/or inspection steps. This can lead to significant reduction in alignment efforts in each of the integrated processing setups and also in a significant reduction of uncertainties associated with the entire hybrid manufacturing sequence. The positioning ARR of the proposed workpiece holding device are carefully assessed in the later sections of the paper.

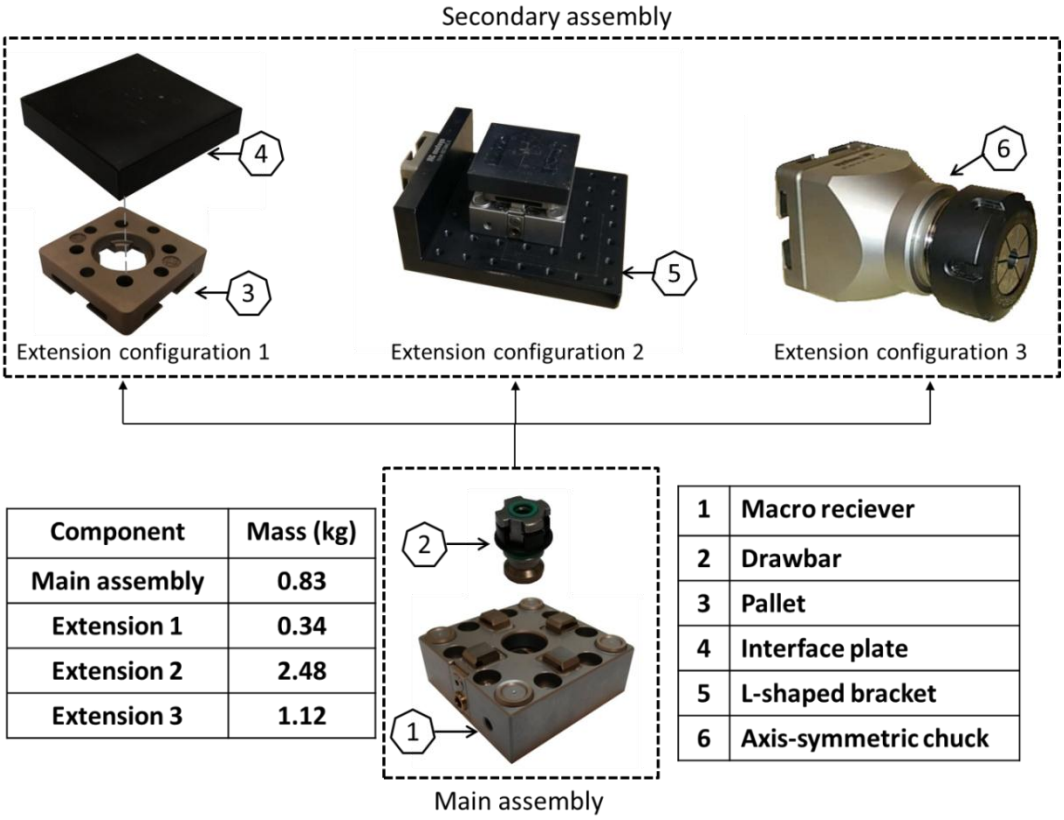

Component	Mass (kg)
Main assembly	0.83
Extension 1	0.34
Extension 2	2.48
Extension 3	1.12

1	Macro reciever
2	Drawbar
3	Pallet
4	Interface plate
5	L-shaped bracket
6	Axis-symmetric chuck

Figure 1. The modular design of the proposed workpiece holding device

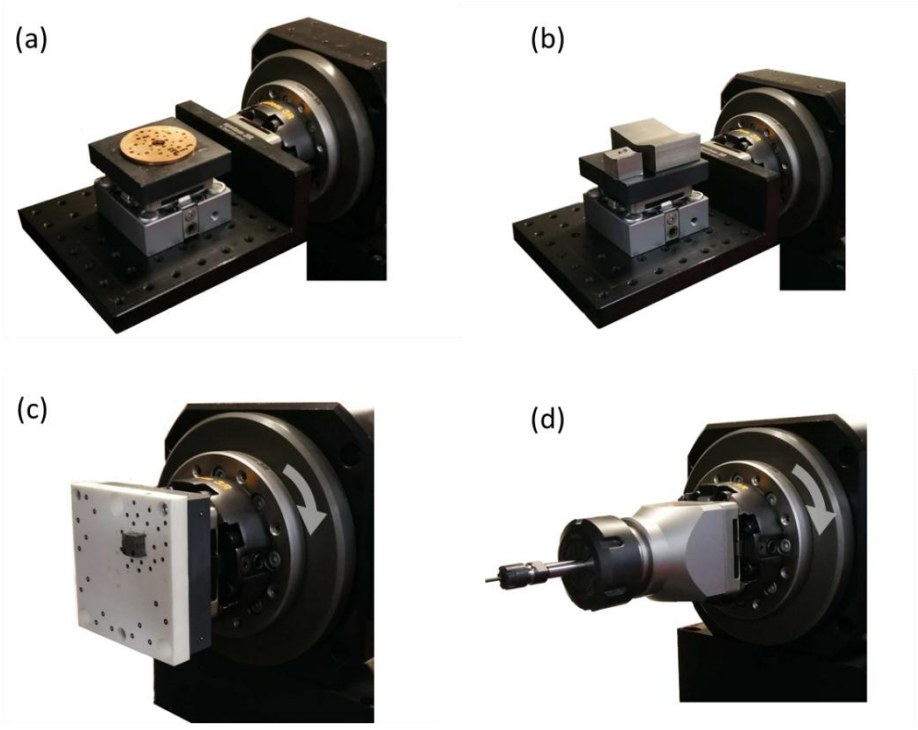

Figure 2. Workpiece holding extensions to realize: (a) one-side processing of a single part; (b) one-side processing of an array of parts; (c) multi-side processing of a single part; (d) machining of axis symmetric parts

3.2 Automated strategies for multi-axis LMM

The implementation of automated multi-axis strategies with rotary stages can broaden significantly the manufacturing capabilities of LMM platforms. For example, such automated strategies are critical for laser polishing of free-form surfaces in order to keep the beam normal and follow the contours of the processed surfaces, and thus to ensure a consistent laser irradiation for uniform polishing results. Furthermore, such an automated tool can also offer an effective solution to address an important intrinsic LMM limitation, namely the side walls tapering of laser machined structures [40], which can affect adversely the parts' functionality. Other applications of such automated strategies include multi-side laser processing of parts (see Figure 2c) and laser processing of axis-symmetric parts (see Figure 2d). The requirements that automated multi-axis LMM strategies should fulfil are:

- to be easily adaptable to the specific requirements of different LMM operations, in particular for machining structures with user-defined side walls taper angle, axis-symmetric parts (Figure 3d) and also parts requiring a multiple-side processing (Figure 3c);
- to provide high machining ARR;
- to take into account changes of the laser beam position in LMM platform coordinate system due to potential laser beam thermal drifts and alignment and calibration issues associated with beam delivery components.

Machine tools standard PD ISO/TR 16907:2015 provides a general outline of machine tool configurations, where machine assembly components are physically linked to the frame of the machine tools through mechanical joints and thus all machine components such as tool spindle and mechanical axes have absolute topologies, determined by the tolerances of the employed mechanical joints, in the machine coordinate system (MCS) [41]. For example, the representation of the kinematic chain diagrams of five-axis milling machines demonstrates that the absolute topological structure of the systems' components in MCS allows the establishment of a structural loop , which maintains the relative positions between a cutting tool and a workpiece throughout the

NC machining commands [42]. Thus, to realise any machining process it is necessary to establish a single geometrical correlation between the MCS and the workpiece coordinate system (WCS) [43]. However, this is not valid in state-of-art LMM machine tool configurations, because they employ both mechanical and optical axes, which are not physically linked and thus possess independent coordinates systems. This is demonstrated in a study where simultaneous utilization of optical axes and a linear stage was only possible after the development of synchronization algorithm, which relies on real time signal transfer between the employed linear stage and the galvanometer scanner [16]. Furthermore, LMM systems incorporate complex beam delivery sub-systems whose component technologies require frequent alignments and calibrations due to the extreme sensitivity of the laser beam pointing stability to environmentally related factors [44]. Such beam positional instabilities lead to beam spot (the laser material interaction area) shifts in the MCS and thus do not allow an absolute topology to be established for laser system component technologies. Therefore, the LMM machine tool configurations should be represented by two coordinate systems, in particular MCS that describes the working volume of the integrated mechanical axes and a beam coordinate system (BCS) that defines the focusing volume covered by the integrated optical axes . Thus, it is necessary to correlate BCS geometrically to the MCS in order to achieve the desired topological laser irradiation of a workpiece. Figure 3 provides a graphical representation of the necessary geometrical correlations between WCS, BCS and MCS that are necessary for executing different LMM operations. In particular, machining results are determined by the geometrical correlation between WCS and BCS that is achieved by referencing both WCS in MCS and BCS in MCS. Since the workpiece is physically attached to the mechanical stages of LMM platforms, WCS is dynamically referenced in MCS and thus any linear or rotary motions of the mechanical stages would maintain the established geometrical correlation of WCS in MCS within the uncertainties associated with the component technologies used to realise their relative movements. However, this is not the case for the geometrical correlation of BCS in MCS because it is assumed to be static due to the absence of a physical link between the laser beam and the mechanical stages. Thus, the execution of

any rotary motions will lead to translational errors in the geometrical correlation of BCS in MCS. These errors after any rotational movements also lead to geometrical misalignments of WCS in BCS and thus to formation of machining errors on the processed workpieces. Therefore, an effective automated strategy for the utilization of rotary stages in LMM platforms ought to include:

- techniques for correlating BCS to MCS, in particular to link BCS to the stages axes of rotations;
- tools for predicting the translational errors in correlating geometrically BCS to MCS after any arbitrary rotary movements;
- corrective commands in the machining routines to compensate the translational errors of BCS in MCS after the execution of rotary movements and thus to ensure high machining ARR.

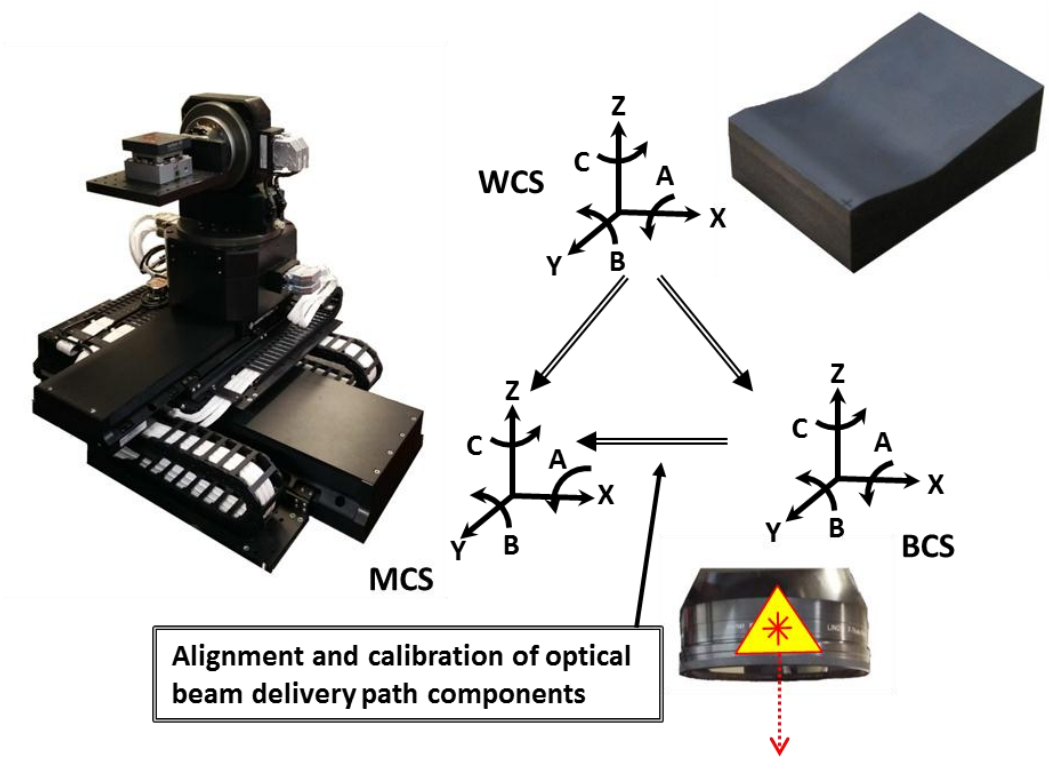

WCS- workpiece coordinate system; BCS- laser beam coordinate system; MCS- machine coordinate system

Figure 3. Geometrical correlations between MCS, BCS and WCS in executing LMM operations

Note: The Right-hand rule notations are used.

3.2.1 Geometrical correlation between BCS and the stages' axes of rotation

Fig. 4a and Fig. 4b depict a method for establishing the geometrical correlation of BCS in relation to the axis of the rotary stages along x and y axes and z axis of a LMM platform, respectively. Points A_0, A_1, A_2,….A_n and Δd_1,…. Δd_n represent the locations of the beam spot in the working plane of the rotary stage and the corresponding distances to its axis of rotation at arbitrary angles, Θ_0, Θ_1, Θ_2,… Θ_n, respectively. Thus, the geometrical correlation of BCS in regards to the axes of the integrated rotary stages can be defined using Equation 1.

$$D_0 = \frac{\sum_{i=0}^{n} \frac{\Delta d_i}{\sin \Theta_i}}{n+1} \qquad \text{Equation 1}$$

It should be noted that the uncertainty of the proposed correlation method reduces with the increase of the number of rotational angles.

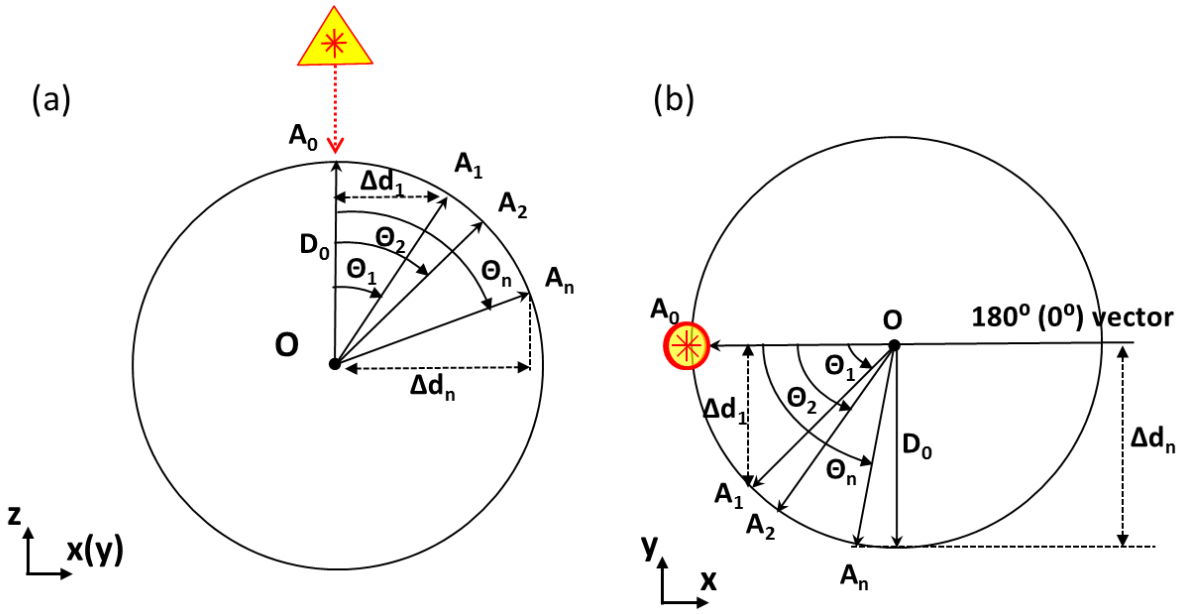

Figure 4. A method for establishing a geometrical correlation between BCS and the axis of a rotary stage about (a) x and y axes and (b) z axis of a LMM platform

3.2.2 Prediction of translational errors

Figure 5 exemplifies the formation of translational errors in correlating geometrically BCS to MCS after any arbitrary rotary movement (Θ) about x and y axes of a LMM platform. Equations 2 and 3 can be used to calculate translational errors, Δy(Δx) and Δz, respectively.

$$\Delta y(\Delta x) = \frac{D_\gamma}{\cos\gamma} \times \sin(\Theta - \gamma) + a \qquad \text{Equation 2}$$

$$\Delta z = D_1 - (\frac{D_1}{\cos\gamma} \times \cos(\Theta - \gamma)) \qquad \text{Equation 3}$$

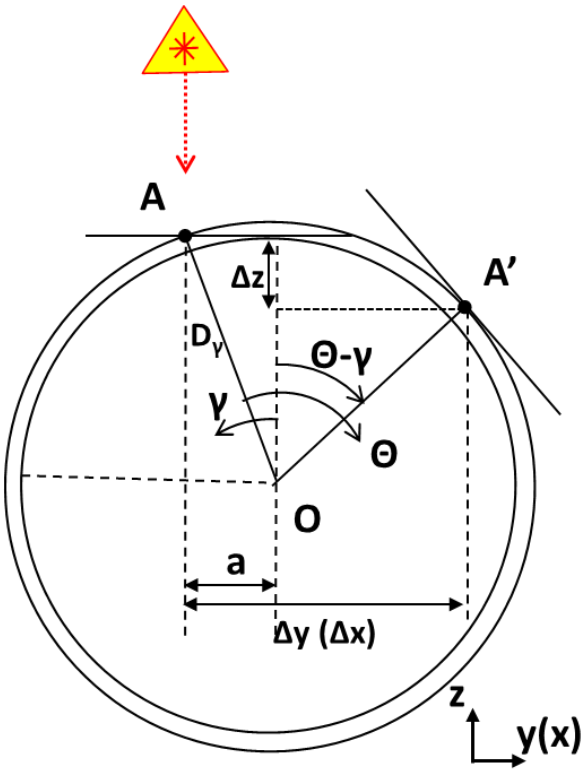

Figure 5. Translation errors in correlating geometrically BCS to MCS after any arbitrary rotary movement about the x and y axes of a LMM platform

Notes: (i) points A and A' represent the initial position (prior to the rotation) and the final position (after the rotation) of the beam spot in MCS, respectively; (ii) point **O** is the centre of rotation of the rotary stage; (iii) **Θ** is the arbitrary angle of rotation; (iv) **a** is the offset distance of beam spot in regards to the axis of rotation along y and x; (v) **γ** is the angle between A and O due to a; (vi) **D_γ** is the distance of point A to the axis of rotation; and (vii) Δy (Δx) and Δz represent the translational errors of the beam spot in MCS due to the rotation along the y(x) axis of the LMM platform.

Figure 6 describes the formation of translational errors in correlating geometrically BCS to MCS after any arbitrary rotary movement (Θ) about the z axis of the LMM platform. Equations 4 and 5 can be used to calculate translational errors Δx and Δy, respectively.

$$\Delta x = \cos(\Omega) \times \frac{b}{\tan(\Omega)} - \cos(\Theta + \Omega) \times D_{\Omega} \qquad \text{Equation 4}$$

$$\Delta y = \sin(\Theta + \Omega) \times D_{\Omega} - b \qquad \text{Equation 5}$$

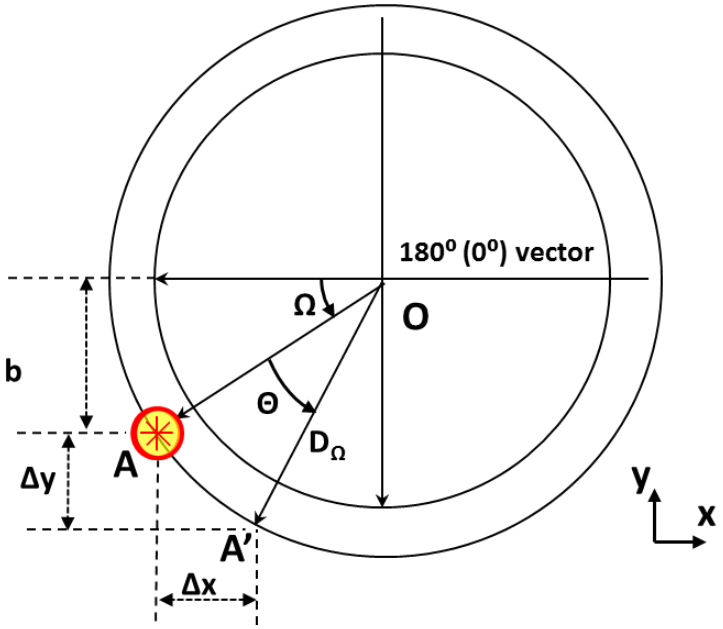

Figure 6. Translation errors in correlating geometrically BCS to MCS after any arbitrary rotary movement (a) about the x and y axes and (b) about the z axis of the LMM platform

Notes: (i) **b** is the offset distance of beam spot in regards to the 0° (180°) vector; (ii) Ω is the angle between 0° (180°) vector and vector OA; and Δx and Δy represent the translational errors of the beam spot in MCS due to the performed rotation along the z axis of the LMM platform.

3.2.3 Corrective commands

Figure 7 provides a schematics representation of the algorithm used to implement a routine for performing laser multi-axis machining with rotary stages. The proposed algorithm is fully automated and introduces corrective commands in the machining routines based on given rotational angles. Furthermore, the algorithm can account for geometrical errors in correlating BCS to MCS caused by

alignments and calibrations of optical components in the beam delivery system and thus to improve the machining ARR.

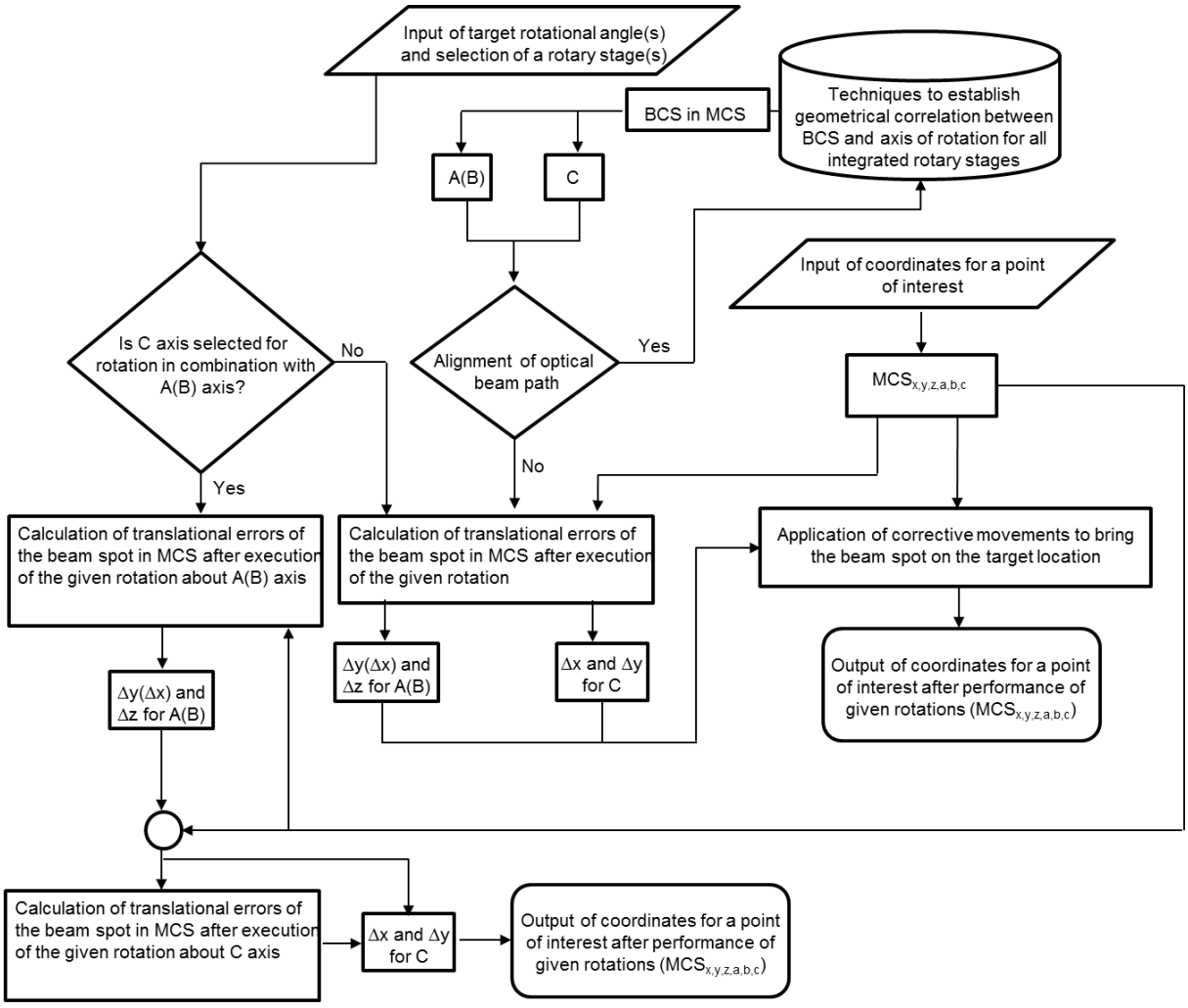

Figure 7. Implementation algorithm for performing laser machining with rotary stages

3.3 Design and implementation of an automated workpiece's setting up routine

The geometrical registration of a workpiece in MCS prior to executing LMM operations is of critical importance in achieving the required level of machining ARR. The common workpieces' settings up routines used in LMM platforms cannot be considered adequate [45]. Important factors that contribute to the high level of uncertainty associated with the widely used workpieces' settings up routines include: the reliance on operators' experience to perform the alignment procedures, the utilization of different component technologies for alignment, such as cameras, confocal probes, and

mechanical contact probes. These factors affect the achievable ARR in correlating WCS to MCS and are a major contributor to the overall ARR in LMM operations. Thus, to minimise the uncertainty associated with the workpieces' settings up routines new tools have to be developed that can address the following requirements:

- flexibly to align work pieces with various geometries;
- minimising/eliminating the influence of workpiece's imperfections, e.g. edge definition and surface integrity, on the alignment results;
- capabilities to link WCS to MCS without the need for pre-existing alignment marks;
- Capabilities to perform non-contact alignment of workpieces and thus to avoid damaging processed surfaces and hence additional uncertainty in executing such routines, especially when polymers are machined or pre-existing micro features that can be easily damaged are used as datum points.
- minimising the influence of the human factor and the need to use experienced operators in conducting the alignment routines.

An automated workpiece's setting up routine is proposed to address these requirements. A schematic representation of this routine is given in Figure 8. It utilizes the Focus Variation (FV) technology [46] and the modular workpiece holding system presented in Section3.1. The installation of the modular workpiece holding device both in a FV system and in the LMM platform establishes the physical link between them and thus the coordinate systems of the FV system (FCS) and MCS can be correlated with a repeatability better then +/- 1 μm (see the experimental validation section of the modular workpiece holding device) and thus can be considered as a single coordinate system of the holding device (HCS). Therefore, through the use of the FV system the geometrical correlation of WCS to HCS can be established that consecutively links WCS to MCS automatically because the correlation between HCS and MCS is already established. The proposed alignment routine is fully automated and this is illustrated in Figure 8. Since the FV system creates a 3D representation of the

workpiece as a cloud of points with uncertainty less than 0.12 μm (when 5x magnification is used) [46], it is possible to capture workpiece imperfections and thus to eliminate their negative effects in linking WCS to MCS. Furthermore, the alignment routine is non-contact and pre-existing micro features can be used without damaging them, and thus eliminates the need for alignment marks on the workpiece. The proposed alignment routine can also increase significantly the throughput of LMM platforms, because the idle times associated with in-situ alignment routines are eliminated. In addition, it is important to stress that the same alignment routine can be used if a FV probe is integrated in the LMM platforms as shown in Figure 9. In this way the uncertainty associated with the routine can be further reduced in expense of the LMM platforms' throughput. Finally, it should be also noted that in-line inspection routines similar to the workpiece's setting up one can be developed for implementing rest-volume machining strategies on LMM platforms [5] and also for generating "customized" toolpaths for adaptive machining [47]. In particular, the adaptive machining approach allows form variations of a workpiece in comparison to its CAD model to be compensated and thus to improve the machining ARR [48].

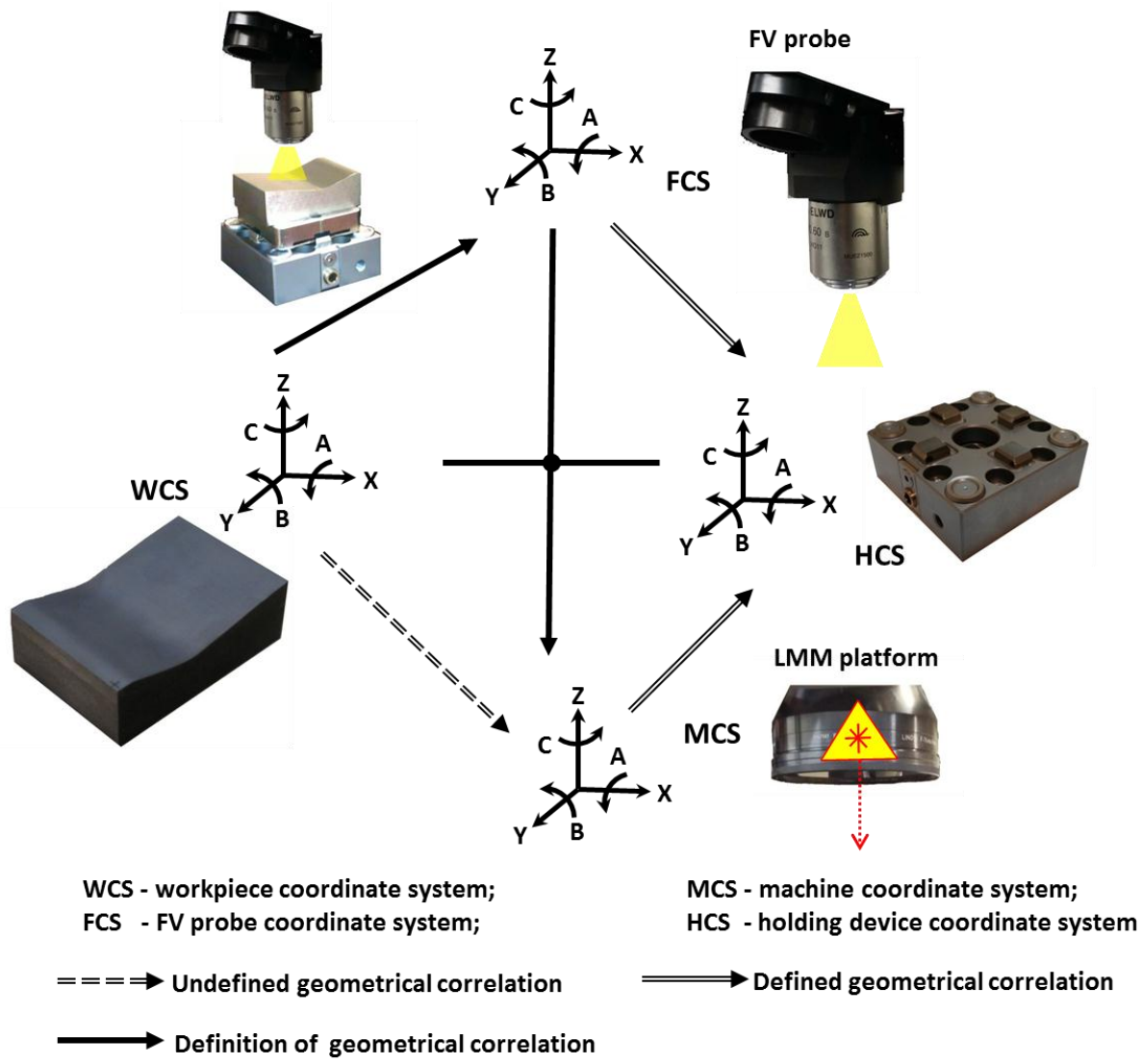

Figure 8. Schematic representation of proposed workpiece's setting up routine

Note: The Right-hand rule notations are used.

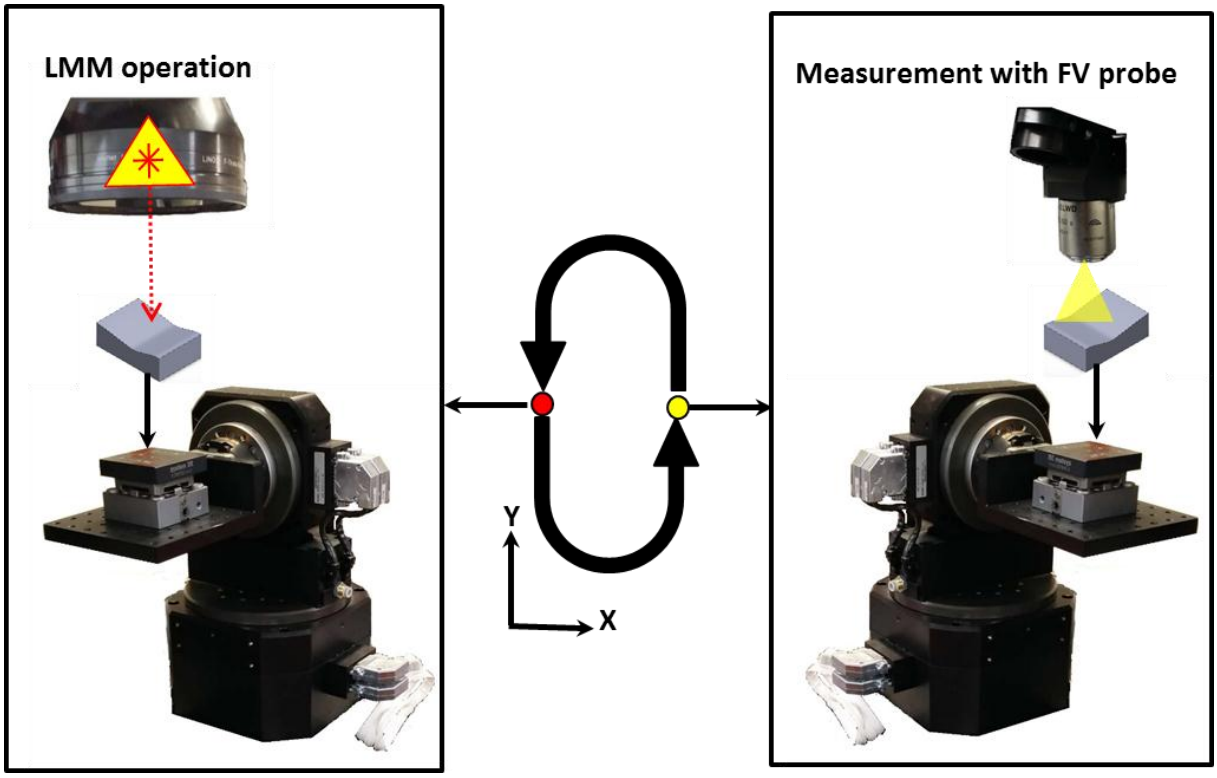

Figure 9. Workpiece's setting up routine with a FV probe integrated into a LMM platform with C rotary stage to swivel between machining and inspection positions

4. Experimental evaluation of the proposed integration techniques/tools

4.1 Equipment and uncertainty considerations

Experimental tests were performed on state-of-art LMM platform, which incorporates three linear stages, two rotary stages and three optical axes for moving the beam spot with high dynamics within 35x35x6 mm processing envelop. The linear and rotary stages used in the experimental validation of the developed tools are commonly integrated in LMM platforms and their positioning resolutions as stated by their manufacturer are 0.25 µm and 45 µrad, respectively [39, 28]. The ARR achievable with the 3D scan head are better than +/- 5 µm across the full range of scanning speeds [18]. The LMM platform integrates two laser sources - a SPI redENERGY G4 S-type 50 W nanosecond (ns) fibre laser that operates at a central wavelength of 1064 nm and supports repetitions rates up to 1 MHz and an Yb-doped femtoseconds (fs) 5W laser sources from Amplitude Systemes that operates at a

central wavelength of 1030 nm and has a maximum repetitions rate of 500 KHz. Also, the LMM platform is equipped with a 100 mm telecentric focusing lens with a machining field of view of 35 mm by 35 mm. The fs laser source and mechanical linear stages are employed in the experiments in order to minimise the uncertainty associated with the LMM operations. In particular, the use of the fs laser improves the edge definition of the machined structures and thus minimises the measurement uncertainty associated with the validation tests. Furthermore, repositioning movements in the LMM tests are performed with the mechanical stages due to their high positioning resolution, better than 0.25 µm. Unless otherwise stated in the experimental procedures, the following laser settings were used to carry out the LMM operations in the experiments: average power of 4.2 W, frequency of 100 kHz, and scanning speed of 500 mm/s. In all tests, the width of the test structures is the same and is determined by the beam spot diameter at the focal plane, in particular, 40 µm at the focal plane.

The FV system employed in the proposed automated workpiece's setting up routine is Alicona G5 [46]. Due to the low resolution required to execute the setting up routine, only x5 magnification was used and the time necessary to scan a volume of 10 mm x 10 mm x 1 mm is only 60s and thus a very good balance between ARR of the operation and the time necessary to complete it can be achieved. The FV technology was also employed to inspect the LMM structures used in the validation tests but with the x20 magnification and measurement uncertainty (U_m) of 0.01 µm [46]. The uncertainty (U_a) related to the employed analysis for quantifying the ARR capabilities of the three proposed integration tools was also calculated based on five repetitions of the experimental procedures. Since, the machining of test structures in the experiments involved the use of mechanical stages, their contribution to the ARR results was accounted for by considering the uncertainty (U_{ct}) related to the employed component technologies. Thus, the expanded uncertainty was calculated as follows:

$$U_e = \sqrt{({U_m}^2 + {U_a}^2 + {U_{ct}}^2)} \quad \text{Equation 6}$$

4.2 Design of Experiments

4.2.1 Modular workpiece holding device

The positioning ARR of the proposed modular workpiece holding device are validated with the test part shown Figure 10. In particular, four equidistantly patterns are produced on an interface plate of the modular workpiece holding device with a spacing between them equal to 50 mm. The pattern consists of five 0.5 mm long crosses, which are positioned along the x and y axes of the LMM platform with the nominal distance between them of 0.6 mm. The relative positioning movements between the crosses were performed with the mechanical stages due to their higher accuracy and repeatability than the optical scanning head. After the laser machining of each cross in the four patterns the pallet was dismounted from the holding device and then mounted back in order to investigate the ARR achievable with the proposed workpiece holding device. The test structures in Figure 10 were machined on one more interface plate in order to evaluate the positioning reproducibility of the proposed modular workpiece holding device. The positioning accuracy was evaluated based on the maximum deviations of the distances between the crosses in comparison to their nominal values of 600 µm. The positional repeatability and reproducibility of the holding device were evaluated by comparing the measured distances between the crosses with the average distances between them that were obtained from the four patterns on one plate and on the two plates, respectively. Thus, positional repeatability and reproducibility of the modular workpiece holding device are evaluated based on results obtained from 40 repositionings of the two plates in the laser micro-machining setup (20 repositionings per sample).

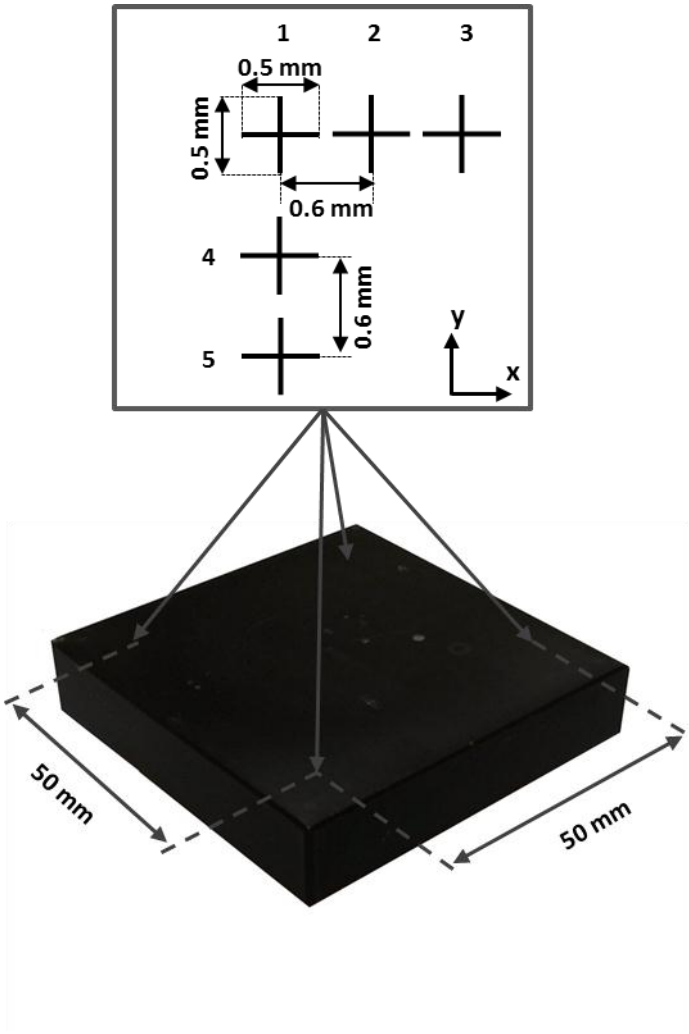

Figure 10. The test plate used to validate positioning ARR of the proposed modular workpiece holding device

4.2.2 Automated strategies for multi-axis LMM

Experimental evaluation of the machining ARR of the proposed automated strategy for multi-axis LMM using rotary stages is performed using the test procedure in Figure 11. The machining ARR achievable when the A and C axes are employed individually are evaluated first with the test procedure in Figure 11a. In particular, a pattern consisting of seven 0.5 mm long crosses that are 0.55 mm apart is machined after pre-defined rotations of both stages. The rotational angles used in the tests are 0^o, +/- 5^o, +/- 10^o and +/- 15^o for both A and C axes, respectively. The pattern in Figure 11a was produced twice per sample and on two samples in order to assess the repeatability and the

reproducibility of the proposed strategy for a single rotary stage. The machining accuracy achievable with either of the two rotary stages (A and C) was assessed based on the maximum displacement of the produced crosses at the pre-defined rotary angles in regards to the reference crosses produced at the home position of the A or C axes ($\Theta=0^o$), respectively. At the same time, the repeatability and reproducibility were evaluated by comparing the displacements of the produced crosses to their average values calculated based on the results from one sample and the two samples, respectively.

The machining ARR when A and C axes are simultaneously utilized, are evaluated by laser machining the pattern in Figure 11b. It consists of five concentric circles whose radiuses increase with an incremental step of 0.1 mm from the innermost circle with a radius 0.25 mm to the outermost circle with a radius of 0.65 mm. Each of the circles is produced after pre-defined simultaneous rotations of both A and C axes. The rotational angles used in the experimental tests are $+/-10^o$ and $+/- 2^o$ for both axes. The pattern from Figure 11b was produced twice per sample and on two samples in order to assess the repeatability and the reproducibility of the proposed strategy for simultaneous utilization of two rotary stages. The machining accuracy achievable with the proposed automated strategy is evaluated by measuring the concentricity of the circles in regards to the reference circle produced at the home position of A and C rotary stages ($\Theta=0^o$). The repeatability and reproducibility were assessed by comparing the concentricity of the circles to their average concentricity values calculated based on the results from one sample and the two samples, respectively. Thus, the repeatability and reproducibility of the proposed automated strategy for multi-axis LMM are evaluated based on 40 test structures produced with the proposed strategy (24 are produced with a single rotary axis and 16 with the simultaneous utilization of two rotary axes).

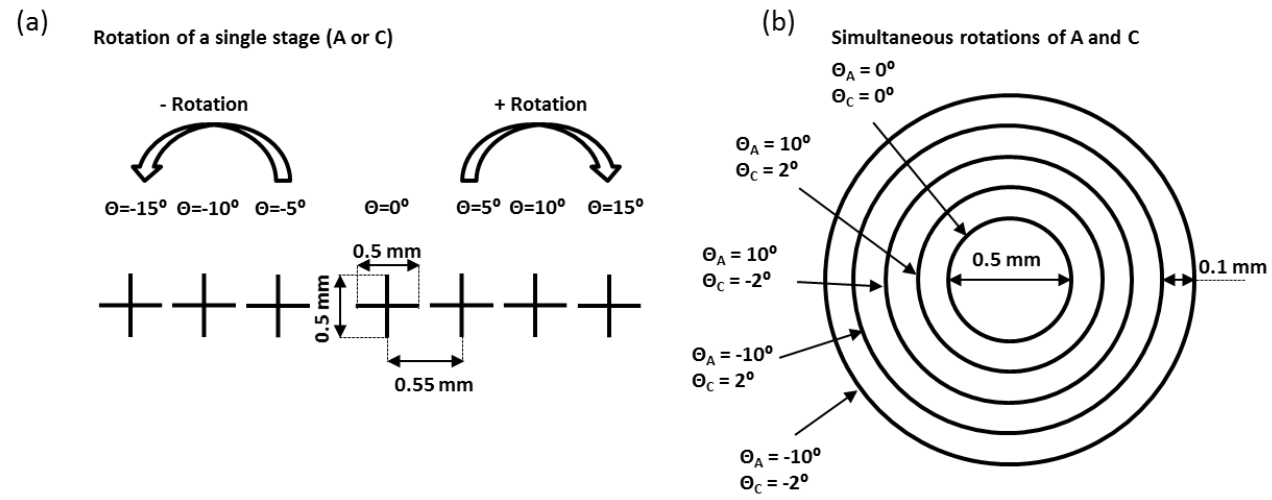

Figure 11. The test procedure used to evaluate the automated strategy (a) the use of a single rotary stage and (b) the simultaneous utilization of A and C rotary stages

4.2.3 *Automated workpiece's setting up routine*

Experimental evaluation of the alignment ARR of the proposed automated setting up routine is performed on a 3D surface of a stainless steel workpiece shown in Figure 12. The overall size of the sample is 60 x 40 mm and LMM is used to texture the 3D surface of the sample with 0.04 mm wide and 0.02 mm deep intersecting trenches, which are 1mm apart and run along the x and y axes of the workpiece. In the absence of pre-existing alignment marks on the wokrpiece, one of the sample corners is used as a WCS origin as shown in Figure 12. The laser machining of each trench on the sample is performed after the workpiece has been dismounted and aligned again with the proposed setting up routine and thus to assess its alignment capabilities. In total, 98 trenches were machined, 59 and 39 along x and y axes, respectively. The processing speed was reduced to 10 mm/s in order to improve the quality of the produced trenches, i.e. their edge definition. The LMM operation was performed on two different workpieces. Since LMM is very sensitive to focal point changes along z axis, the beam propagation direction, any depth and width deviations of the trenches along the 3D surface were used to judge about the alignment capabilities of the proposed routine along the z axis At the same time, the lateral (X-Y plane) alignment accuracy was assessed based on the overall

deviations of the relative distances between trenches in comparison to the nominal value of 1 mm. The lateral repeatability and reproducibility of the proposed alignment routine were evaluated by comparing the measured distances between trenches to their average values obtained from the inspected regions on one sample and on the two samples, respectively. Thus, the repeatability and reproducibility of the proposed automated workpiece's setting up routine are evaluated based on results obtained from 196 repetitions of the alignment strategy (98 alignments per sample).

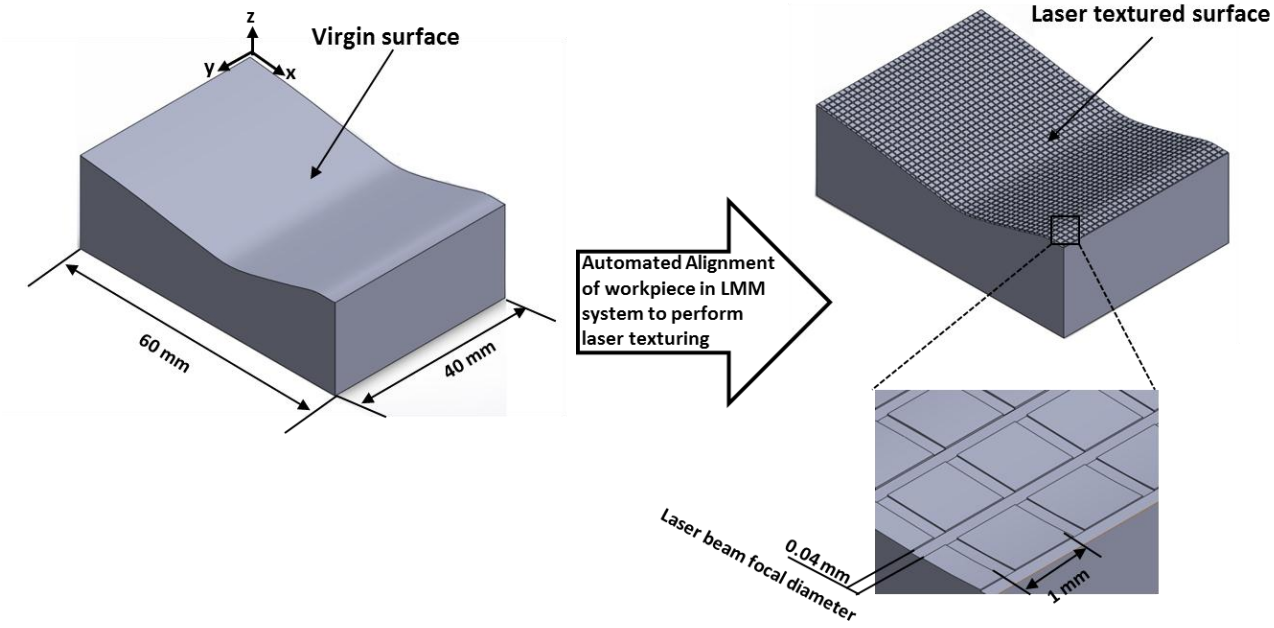

Figure 12. Laser textured test part used to validate the proposed workpiece's setting up routine

5. Results and Discussions

5.1 Modular workpiece holding device

Figure 13a shows one of the laser produced patterns on the interface plate of the workpiece holding device and also the measurements carried out to assess the positioning ARR of the device. In particular, D_1, D_2, D_3, and D4 are the relative distances between crosses 1 and 2, 2 and 3, 1 and 4, and 4 and 5, respectively. Also, Figure 13b shows how one single measurement of the relative

distance between crosses 1 and 2 (D_1) is completed using the Parallel Line Automatic tool of the Alicona G5 2DImageMerasurment module [49]. The automatic tool was used due to the high accuracy and repeatability of the carried out measurements. Table 3 provides the results for the four patterns on the two interface plates and each of them is the average value of five measurements as prescribed in the guidelines for assessing machine tools uncertainty budgets [50]. In particular, Table 3 provides the measured distances together with their corresponding deviations from the nominal value of 600 μm and the calculated average values calculated based on the results from each sample and from both together. The positioning ARR capabilities of the proposed workpiece holding device are assessed based on the analytical procedure provided in Section 4.2.1. It can be seen in Table 3 that the positioning accuracy of the proposed workpiece holding device is 0.85 μm, 0.75 μm, 0.75 μm and 0.95 μm and 0.90 μm, 1.00 μm, 0.55 μm and 0.75 μm for Patterns 1, 2, 3 and 4 on the two plates, respectively. Thus, it can be stated that the positional accuracy of the proposed modular wokrpiece holding device is better than 1.00 μm. The positional repeatability based on the average measured distances calculated from Sample 1 and 2, 599.55 μm and 599.95 μm, is 1.2 μm and 1.05 μm, respectively, and thus it is better than 1.2 μm. At the same time, the average measured distance value for the two plates is 599.87 and therefore the positioning reproducibility of the proposed workpiece holding device is better than 1.1 μm. Since the mechanical stages are used to execute repositioning movements between the crosses, their positional resolution should be also included in the uncertainty calculations when quantifying the ARR capabilities of the workholding device. In particular, by taking into account the uncertainty related to the stages' movements (U_s) of 0.25 μm [31], the expanded uncertainty (U_e) is 0.3 μm. Overall, it can be stated that the positioning ARR of the proposed workpiece holding device including the expanded uncertainty are better than +/- 1.0 μm.

Table 3. Results from experimental testing of the modular workpiece holding device

Plate 1 – Pattern 1 (bottom left)				
	D_1	D_2	D_3	D_4
Nominal distance (μm)	600			
Measured distance (μm)	599.35	599.15	600.35	599.45
Deviation (μm)	-0.65	-0.85	0.35	-0.55
Plate 1 – Pattern 2 (bottom right)				
Nominal distance (μm)	600			
Measured distance (μm)	600.50	600.15	600.75	599.35
Deviation (μm)	0.50	0.15	0.75	-0.65
Plate 1 – Pattern 3 (top left)				
Nominal distance (μm)	600			
Measured distance (μm)	599.30	599.25	600.35	600.45
Deviation (μm)	-0.70	-0.75	0.35	0.45
Plate 1 – Pattern 4 (top right)				
Nominal distance (μm)	600			
Measured distance (μm)	599.50	599.65	600.15	599.05
Deviation (μm)	-0.50	-0.35	0.15	-0.95
Average measured distance for Sample 1 (μm)			599.55	
Plate 2 – Pattern 1 (bottom left)				
	D_1	D_2	D_3	D_4
Nominal distance (μm)	600			
Measured distance (μm)	599.10	599.25	599.35	599.95
Deviation (μm)	-0.90	-0.75	-0.65	-0.05
Plate 2 – Pattern 2 (bottom right)				
Nominal distance (μm)	600			
Measured distance (μm)	601.00	600.15	600.45	599.85
Deviation (μm)	1.00	0.15	0.45	-0.15
Plate 2 – Pattern 3 (top left)				
Nominal distance (μm)	600			
Measured distance (μm)	600.50	599.45	600.05	599.75
Deviation (μm)	0.50	-0.55	0.05	-0.25
Plate 2 – Pattern 4 (top right)				
Nominal distance (μm)	600			
Measured distance (μm)	600.20	600.65	600.25	599.25
Deviation (μm)	0.20	0.65	0.25	-0.75
Average measured distance for Sample 2 (μm)			599.95	
Average measured distance for the two plates (μm)			599.90	

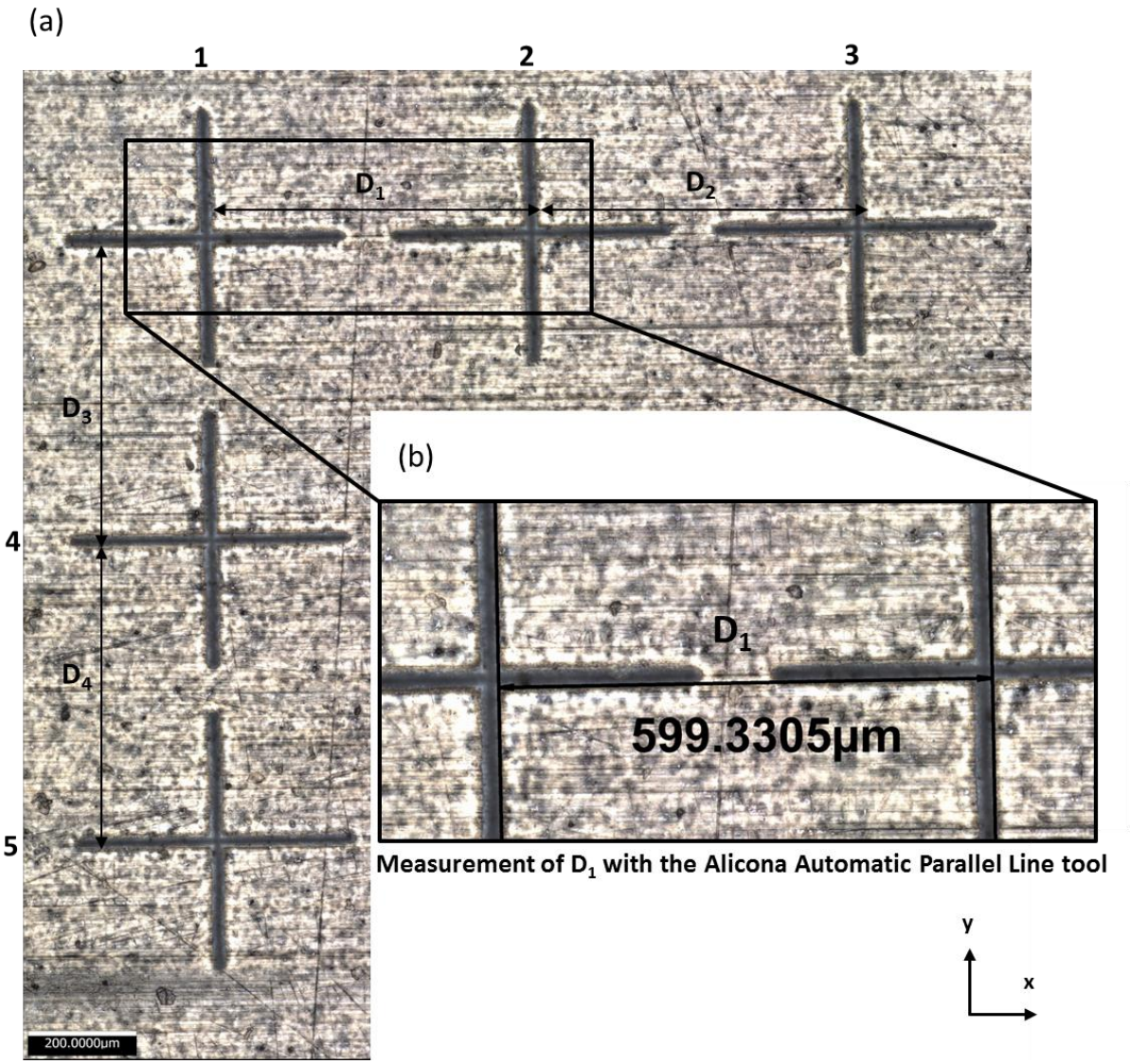

Figure 13. Laser machined Pattern 1 on the first interface plate: (a) a view of the complete pattern and (b) close view of two crosses from the machined pattern

5.2 Automated strategies for multi-axis LMM

Figure 14a shows the top view of the crosses produced after completing the test procedure described in Section 4.2.2. The central cross in Figure 14a is produced at $\Theta_A = 0^o$ and it is used as a reference to quantify the displacements (Δd) of other crosses produced after executing pre-defined rotations with the A rotary stage. The displacements of the crosses were calculated by using the Alicona Contour tool [49] as shown in Figure 14b. In particular, the crosses' contours were extracted and then automatic fitting of parallel lines was applied on the respective edges as shown in Figure

14c. In this way, their displacements are quantified to assess the effectiveness of the corrective commands when executing multi-axis machining strategies with a single rotary stage. For example, the measurement procedure used to assess the accuracy of the applied corrective command after a rotation of -5 degrees with the A axis is illustrated in Figure 14c. The results from the tests carried out for both A and C axes are provided in Table 4. The positioning ARR capabilities of the proposed multi-axis machining strategies with a single rotary stage are assessed based on the analytical procedure provided in Section 4.2.2. It can be seen in Table 4 that the maximum displacement of the crosses produced with the A axis are 5.4 μm and 5.3 μm and 4.2 μm and 4.1 μm for Patterns 1 and 2 on the two samples, respectively. At the same time, the maximum overall displacements of the crosses produced with the C axis are 5.7 μm and 4 μm and 4.9 μm and 5.0 μm for Patterns 1 and 2 on the two samples, respectively. Thus, it can be stated that the accuracy achievable with the proposed strategy for multi-axis LMM employing either A or C axes is better than 5.7 μm. The repeatability of the proposed strategy with the A axis is 5.3 μm and 3.8 μm for Samples 1 and 2, respectively, based on average displacements in Table 4. Since, the machining of the crosses with the proposed strategy using the C axis required corrective commands with x and y components, the repeatability is assessed taking into account the displacements both along x and y axes. Figure 15 shows the distribution of the crosses' displacements in regards to the average displacements for the two samples, respectively, and thus the repeatability of the proposed strategy using the C axis is 6.4 μm and 6.2 μm for Samples 1 and 2, respectively. Based on these results, it can be stated that the repeatability of multi-axis LMM employing either A or C axes is better than 6.4 μm. At the same time, the reproducibility of the proposed strategy is 5.0 and 5.9 μm using the A and C axes, respectively, based on the average displacements of the crosses in Table 4 and Figure 15. The expanded uncertainty in quantifying the ARR capabilities of the proposed strategy for multi-axis LMM with either A or C axes can be calculated using Equation 6 and it is 0.46 μm.

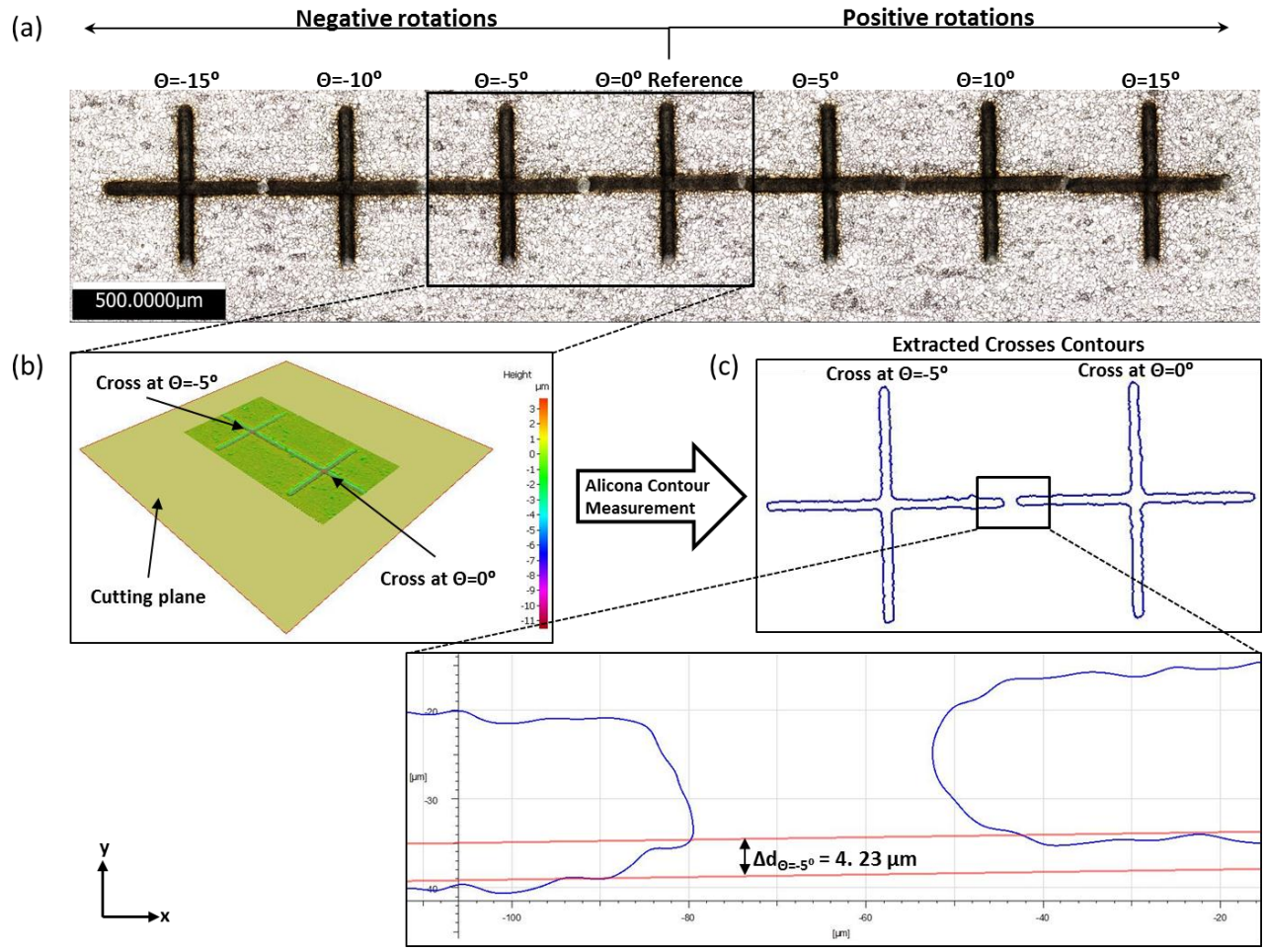

Figure 14. Laser machined crosses with the proposed automated strategy when A axis is used only, (a) top view of the crosses for all investigated rotational angles, (b) application of Alicona Contour tool on crosses produced at $\Theta_A = 0^o$ and $\Theta_A = -5^o$, (c) extracted crosses contours and measurement of the positional deviation of the cross at $\Theta_A = -5^o$ in comparison to the cross at $\Theta_A = 0^o$

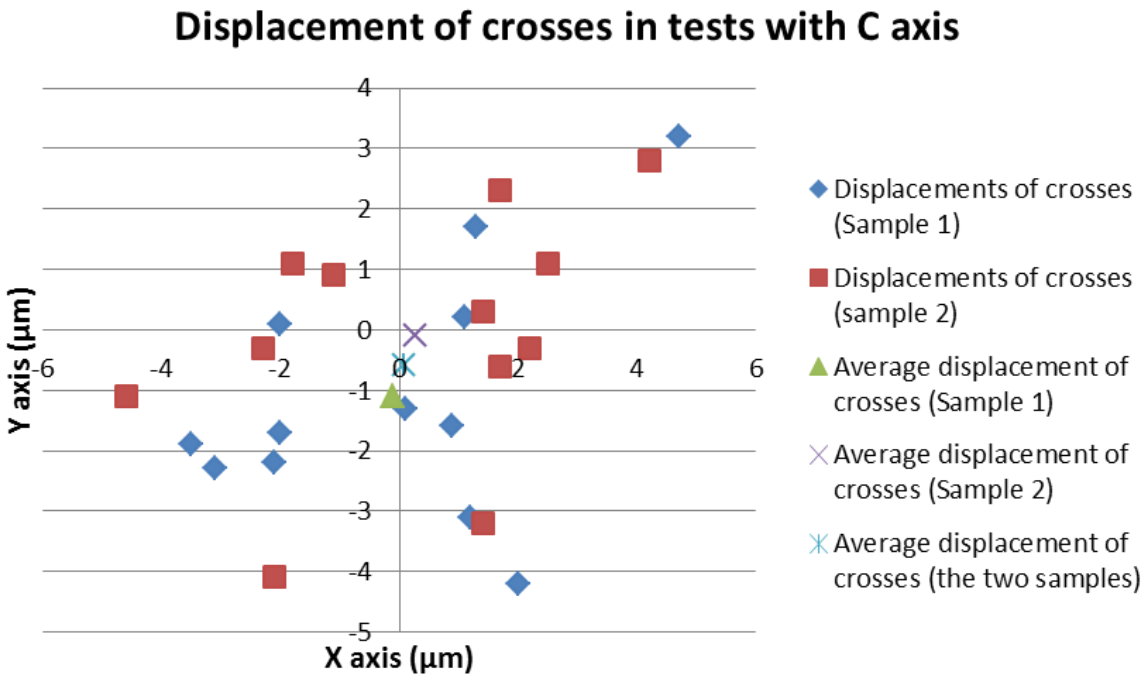

Figure 15. Repeatability and reproducibility of the proposed strategy using the C axis

Table 4. Test results after using the A and C rotary stages separately

Parameter	**Sample 1 – Pattern 1 - A axis**						**Sample 1 – Pattern 2 - A axis**					
Rotary angle (°)	5	10	15	-5	-10	-15	5	10	15	-5	-10	-15
Displacement-x axis (µm)	-	-	-	-	-	-	-	-	-	-	-	-
Displacement-y axis (µm)	5.4	5.1	-2.7	-4.2	-1.9	5.1	5.3	4.1	0.5	-2.6	-4.2	3.7
Average displacement for Sample 1- A axis (µm)	1.1											
Parameter	**Sample 2 – Pattern 1 - A axis**						**Sample 2 – Pattern 2 - A axis**					
Rotary angle (°)	5	10	15	-5	-10	-15	5	10	15	-5	-10	-15
Displacement-x axis (µm)	-	-	-	-	-	-	-	-	-	-	-	-
Displacement-y axis (µm)	-2.1	3.7	-2.3	-1.2	4.2	2.1	1.1	4.1	-1.3	-1.6	-2.2	0.7
Average displacement for Sample 2 – A axis (µm)	0.4											
Average deviation for the two samples – A axis (µm)	**0.8**											
Parameter	**Sample 1 – Pattern 1 - C axis**						**Sample 1 – Pattern 2 - C axis**					
Rotary angle (°)	5	10	15	-5	-10	-15	5	10	15	-5	-10	-15
Displacement-x axis (µm)	1.2	-3.1	-2.0	2.0	-3.5	4.7	0.1	-2.0	1.1	0.9	-2.1	1.3
Displacement-y axis (µm)	-3.1	-2.3	-1.7	-4.2	-1.9	3.2	-1.3	0.1	0.2	-1.6	-2.2	1.7
Overall absolute displacement (µm)	3.3	3.9	2.6	4.7	4.0	5.7	1.3	2.0	1.1	1.8	3.0	2.1
Parameter	**Sample 2 – Pattern 1 - C axis**						**Sample 2 – Pattern 2 - C axis**					
Rotary angle (°)	5	10	15	-5	-10	-15	5	10	15	-5	-10	-15
Displacement-x axis (µm)	2.2	-1.1	-1.8	1.4	-2.3	1.7	1.4	-4.6	2.5	1.7	-2.1	4.2
Displacement -y axis (µm)	-0.3	0.9	1.1	-3.2	-0.3	2.3	0.3	-1.1	1.1	-0.6	-4.1	2.8
Overall absolute displacement (µm)	2.2	1.4	2.1	3.5	2.3	2.9	1.4	4.7	2.7	1.8	4.6	5.0

Figures 16a and 16b show the top and 3D view of the circles produced with the proposed automated strategy that required the simultaneous utilization of both A and C axes of the LMM platform. The experimental validation of the proposed tool is performed by measuring the concentricity of the circles produced following the test procedure in Section 4.2.2. In particular, the concentricity of C2, C3, C4 and C5 were measured in respect to C1 produced at $\Theta_A = \Theta_C = 0^o$ as shown in Figure 16c. Figure 17 provides a plot with the results and it can be stated that accuracy of the proposed strategy with simultaneous utilization of A and C axes is better than 10.6 µm. Furthermore, the repeatability of the proposed strategy is better than 10.9 µm and 10.8 µm for Samples 1 and 2, respectively, while the reproducibility is better than 12.6 µm. The expanded uncertainty for quantifying the ARR capabilities of the proposed strategy is 0.53 µm. Based on these results, it can be stated that the machining ARR achievable with the proposed multi-axis LMM strategy with the simultaneous use of the A and C rotary stages including the expanded uncertainty are better than +/-6.5 µm.

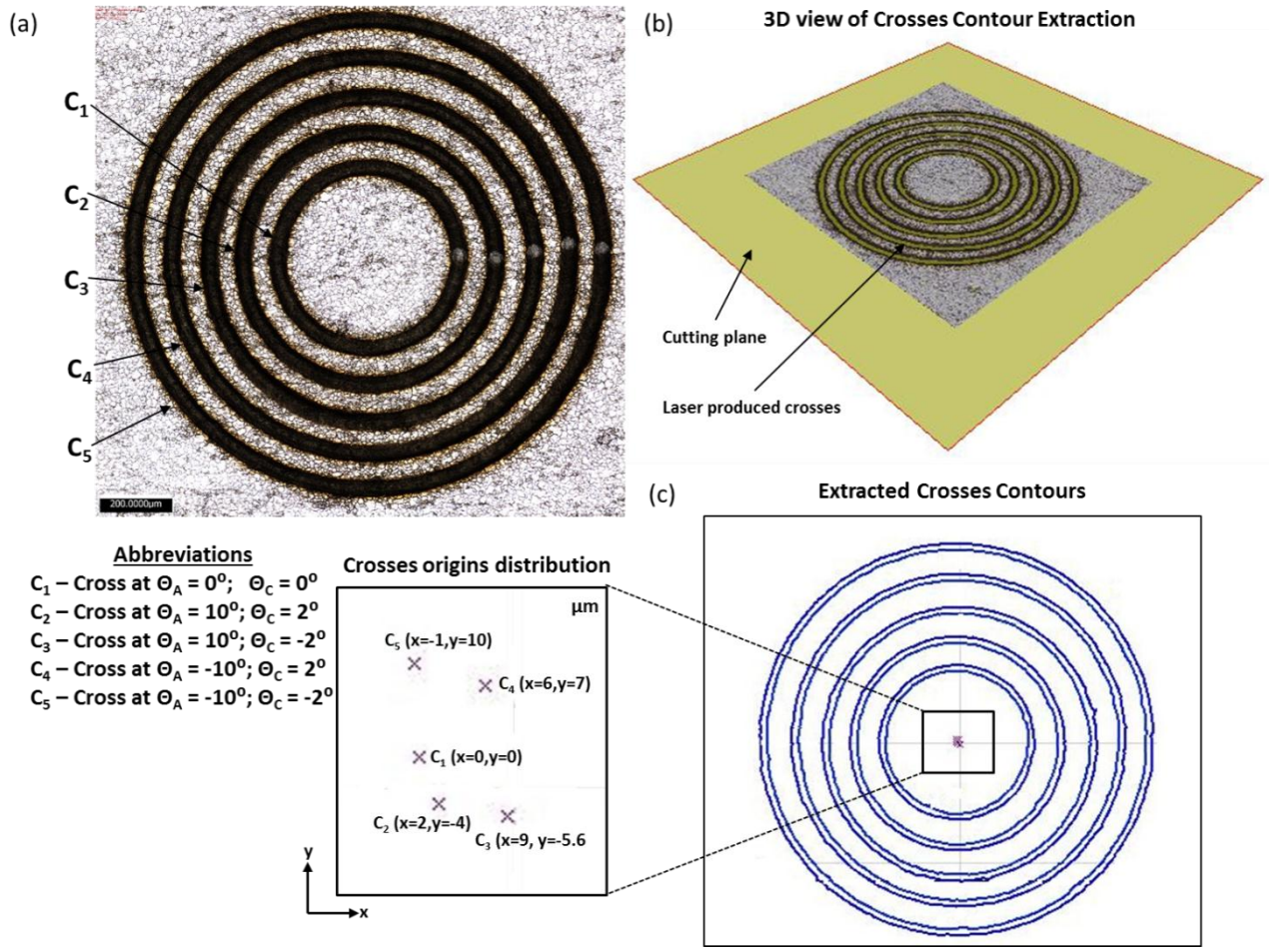

Figure 16. The circles machined with the proposed automated strategy with the simultaneous utilization of the A and C axes: (a) Top view of the circles; (b) 3D view of the circles generated with Alicona Contour tool; and (c) extracted circles' contours with the procedure for measuring their concentricity

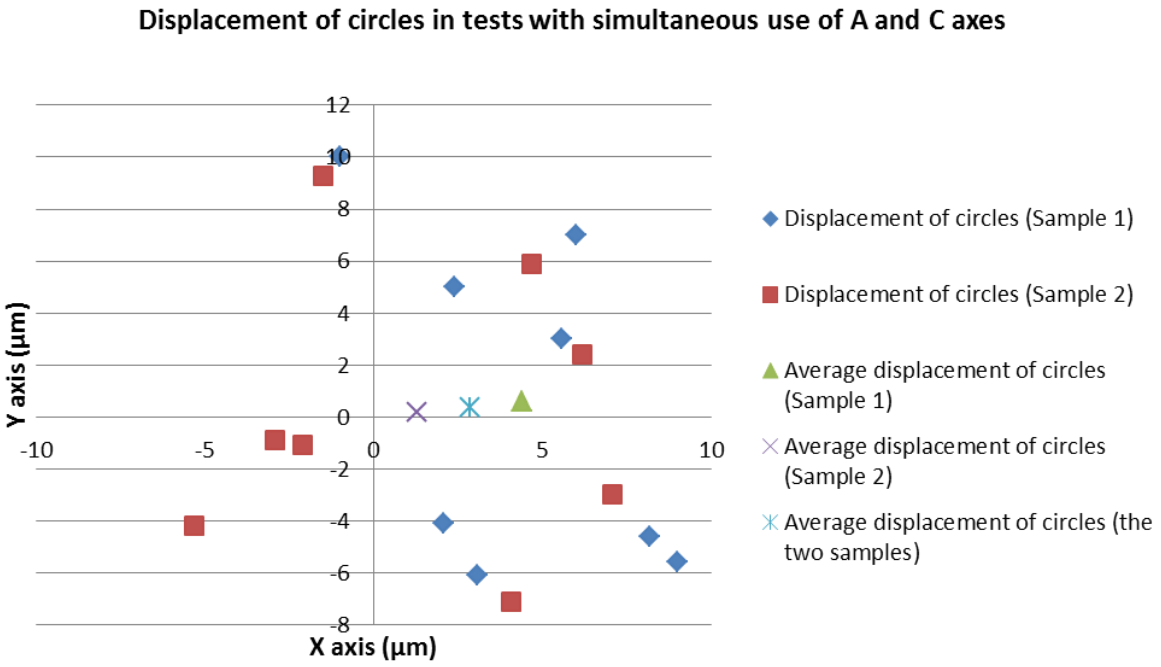

Figure 17. Repeatability and reproducibility of the proposed strategy with simultaneous utilization of A and C axes

5.3 Automated workpiece's setting up routine

Figure 18a shows a cloud of points representing the 3D surface of a sample prior to the laser texturing operation, while Figure 18b provides a close view of one of the sample edges, where workpiece imperfections such as roughness, waviness and edge definition are clearly visible. Such workpiece imperfections affect the achievable alignment accuracy with manually executed setting up routines when high resolution optical cameras are employed. In contrast, the proposed alignment routine scans the complete sample and thus takes into account the wokrpiece imperfections and minimises their effects on alignment accuracy and precision. Figure 19 shows a scan field of the laser textured 3D surface, where the test procedure applied to validate the proposed workpiece setting up routine is also depicted. In particular, P_i represent the points at which the depth and width profiles of the trenches are analysed, while I_i represent the intersection points between the trenches used to evaluate the lateral alignment accuracy. An example of the carried out profile analysis is given in Figure 20 where the width and depth of a single trench at three P_i are provided. LMM

operations are very sensitive to any offsets of the focal points from the workpiece surface which results in variations of the depth and width of the trenches along the 3D surface. There are two main factors contributing to this offset, in particular the alignment accuracy and the dynamics of the Z optical axis, especially the moving lens used to realise it. The scanning speed during the laser texturing operation in this test was reduced to 10mm/s to minimise the effects of this factor. Consequently, the good profile uniformity of the trenches along the 3D surface can be attributed mostly to the capability of the proposed setting up routine. The total number of analysed trenches is six, three along the x and y axes, and thus the total number of P_i inspected is 18. Figure 21 provides a plot with the performed analysis of all 12 trenches machined on the two samples. Based on these results it can be stated that the maximum deviation of the widths and the depths of the trenches on the two samples do not exceed **+/- 5** μm and thus this demonstrates the accurate and repeatable alignment along the z axis of the LMM platform.

Furthermore, a quantitative evaluation of the lateral alignment ARR achieved with the proposed setting up routine is also performed by measuring the distances between individual trenches at the intersection points, I_i, as shown in Figure 22. In particular, the relative distance between the trenches is measured and then compared with their nominal values to judge about the alignment accuracy of the proposed setting up routine. For example, the alignment accuracy shown in Figure 22 is 5.3 μm and 2.5 μm along the y and x axes, respectively. The total number of intersection points investigated per sample is four and the results are provided in Table 5. The maximum overall deviation of the relative distances between the trenches for the two machined samples is 7.4 μm and thus it can be stated that the lateral alignment accuracy is better than 7.4 μm. Thus, taking into account the average values in Table 5 the lateral alignment repeatability achieved for Sample 1 and 2 are 5.8 μm and 7.3 μm, respectively, while the lateral alignment reproducibility is better than 6.9 μm. The expanded uncertainty of the alignment routine is 0.7 μm. Based on these results, it can be stated that the lateral alignment ARR achievable with the proposed workpiece setting up routine including the expanded uncertainty are better than +/-4.0 μm.

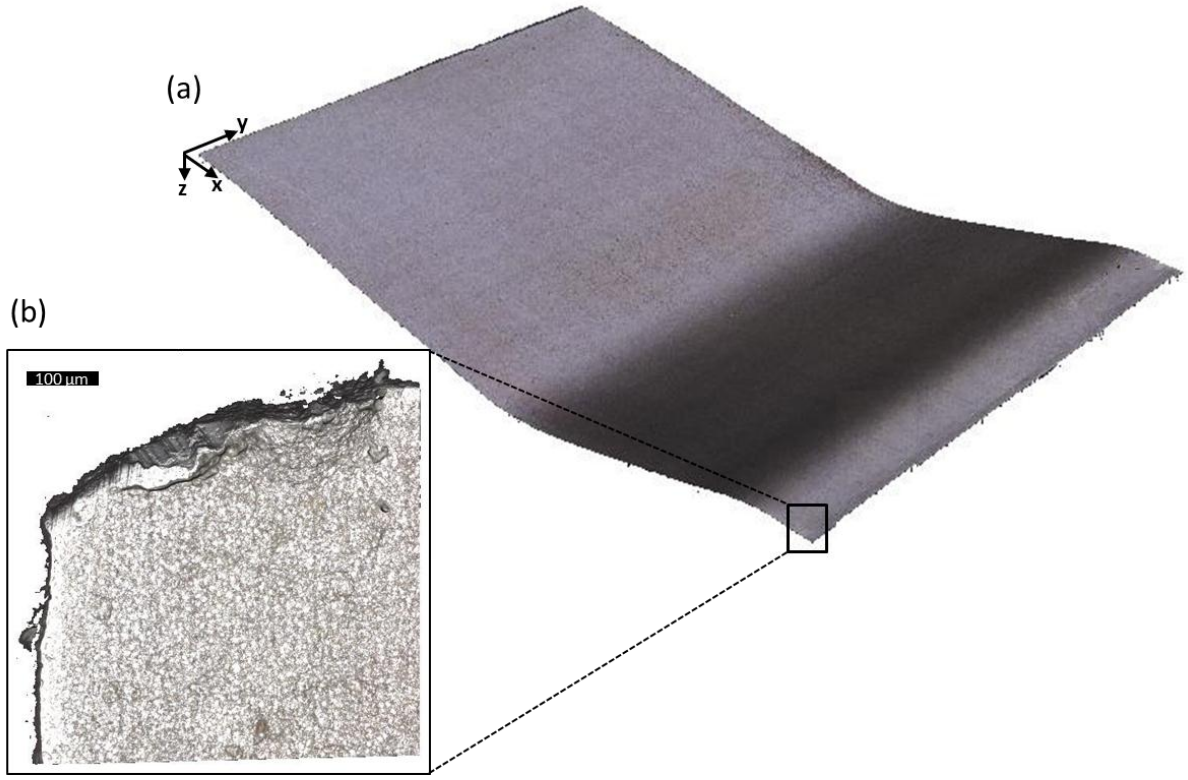

Figure 18. The scan results obtained with the FV system: (a) 3D surface of the sample workpiece represented as a cloud of pints and (b) a close view of a sample edge.

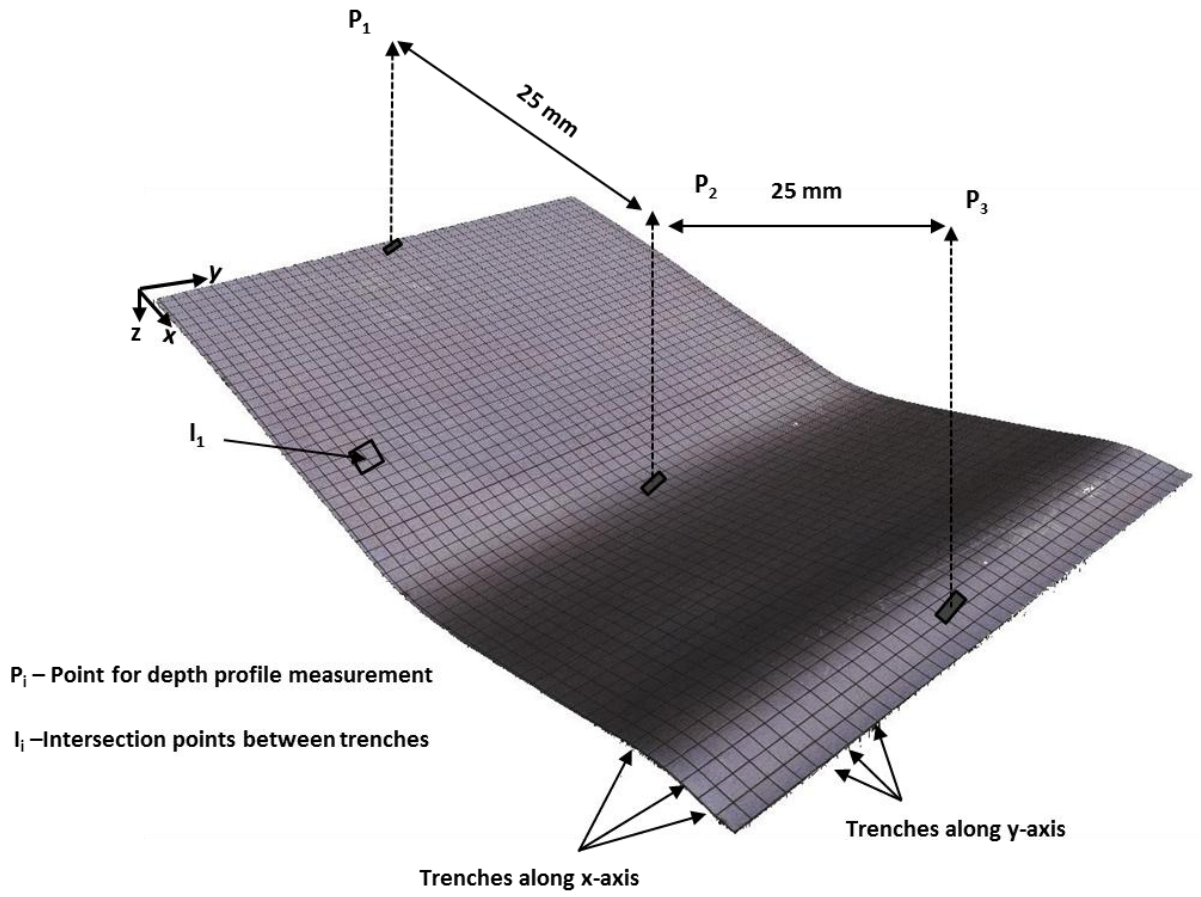

Figure 19. Laser textured surface represented as a cloud of points acquired with the FV system

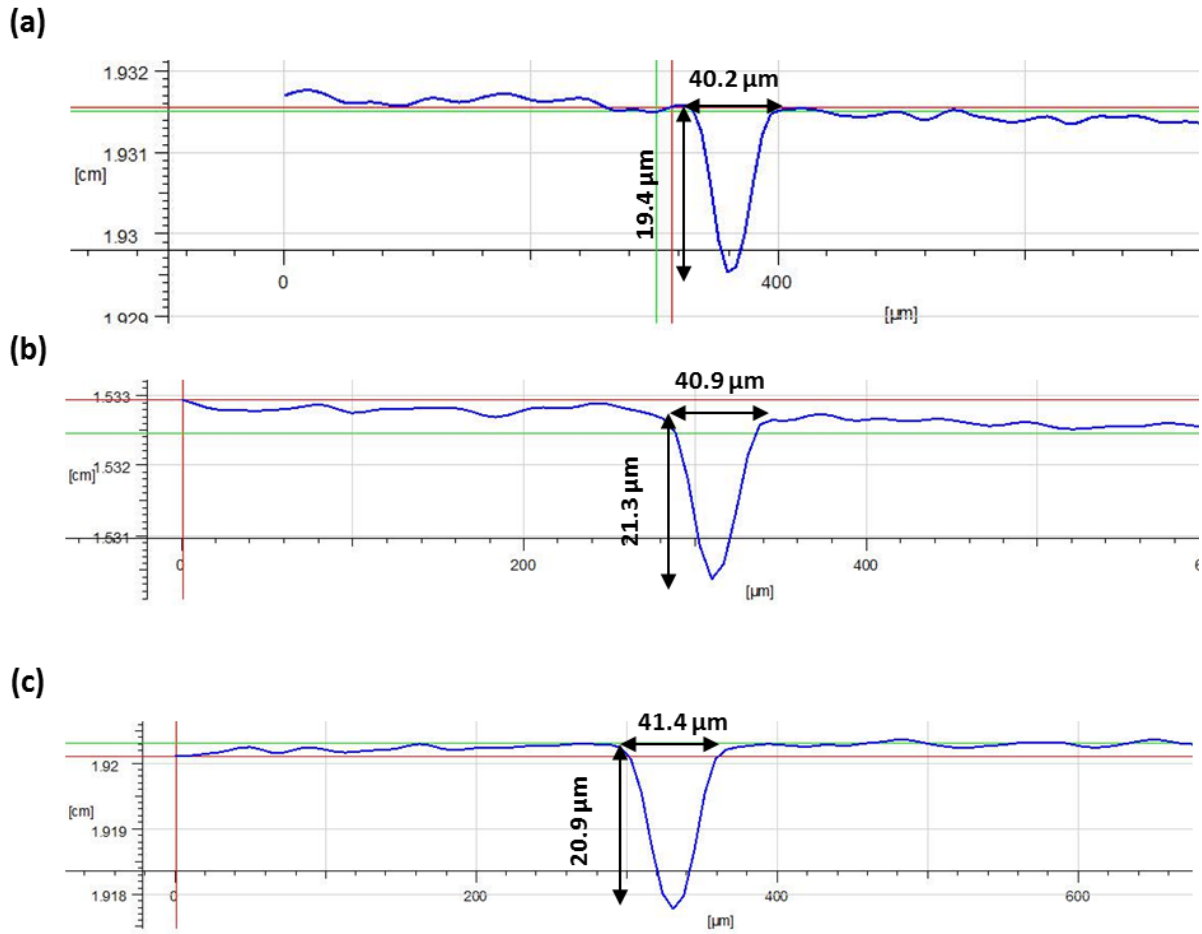

Figure 20. Depth and width profiles at three different points on a single trench: (a) point 1 (P_1), (b) point 2 (P_2) and (c) point 3 (P_3)

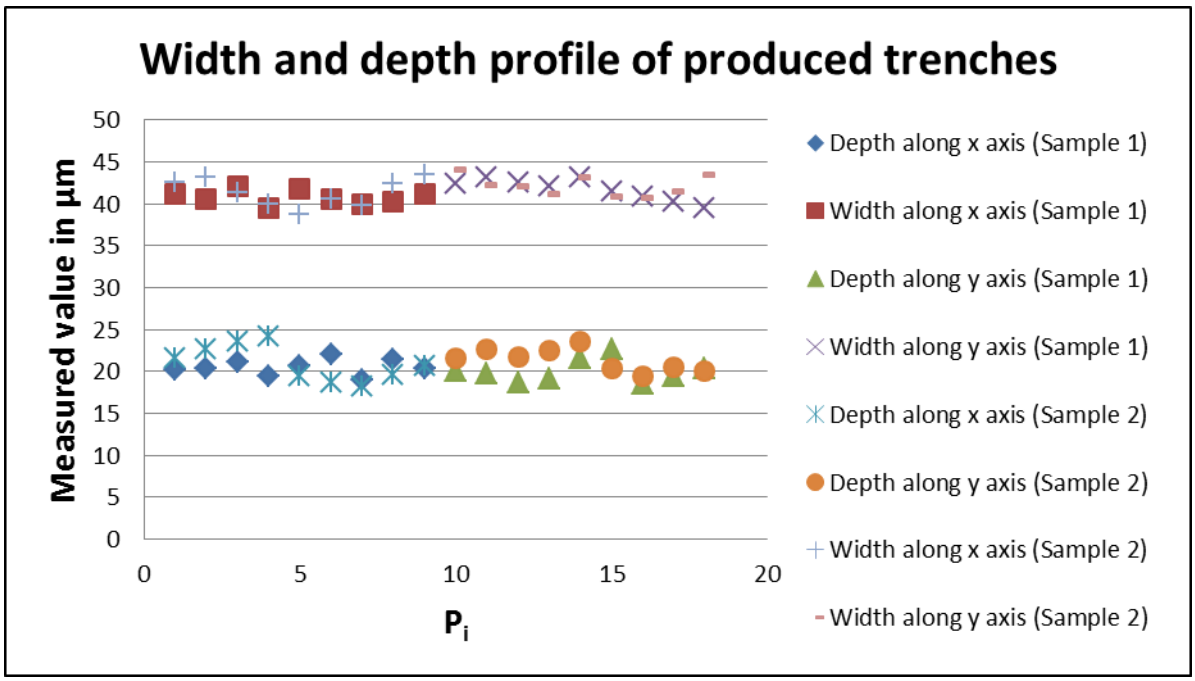

Figure 21. Results for the six trenches per sample analysed on the two samples

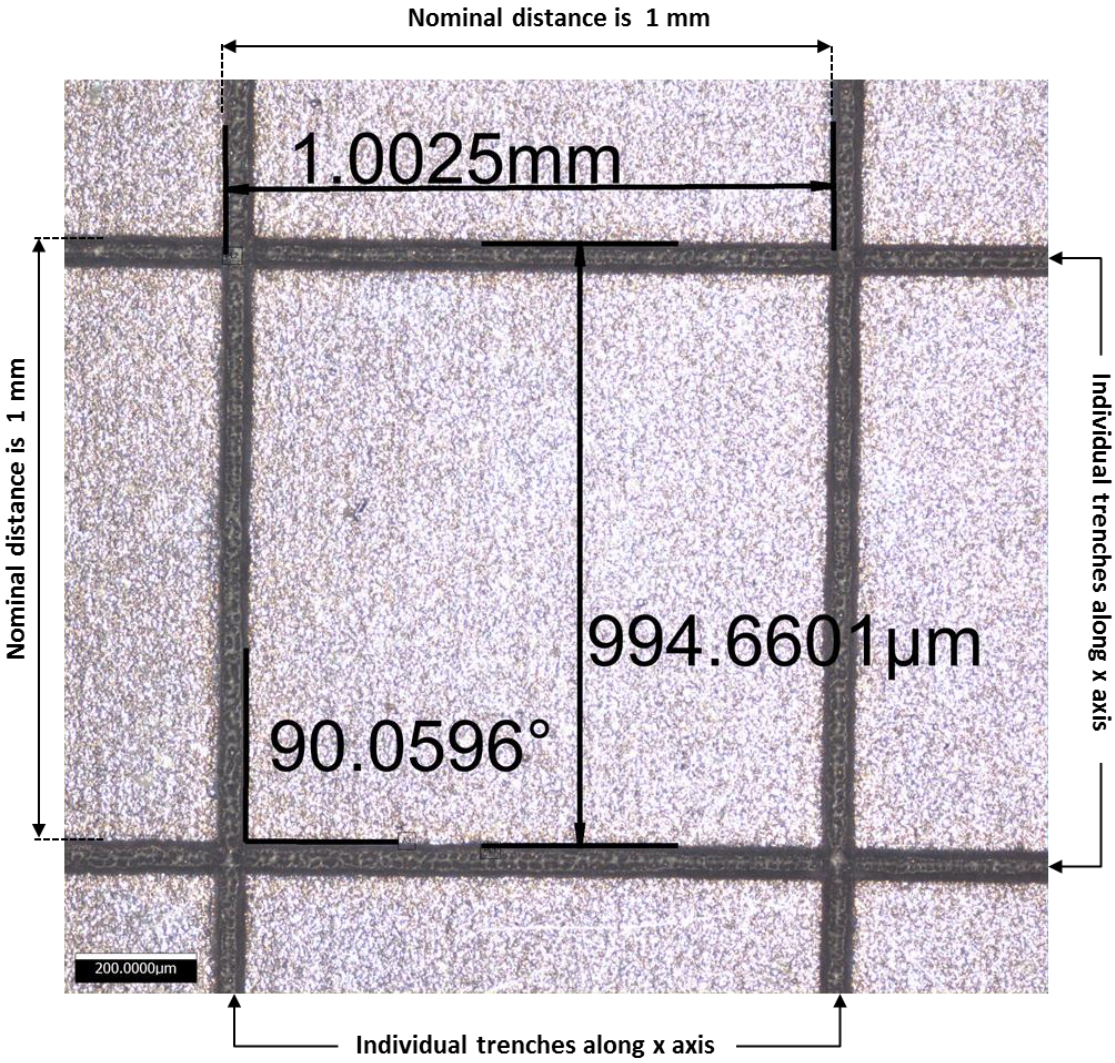

Figure 22. The measurements of distances between the trenches at an intersection point

Table 5.Measurments of relative distances between the trenches in regards to their nominal values

Parameter	Sample 1				Sample 2			
Intersection Point	I_1	I_2	I_3	I_4	I_1	I_2	I_3	I_4
Nominal Length (x-axis) (µm)	1000							
Measured Length (x-axis)(µm)	1002.5	1001.6	998.2	1003.2	1003.1	1004.2	997.6	1006.1
Deviation-x axis (µm)	2.5	1.6	-1.8	3.2	3.1	4.2	-2.4	6.1
Nominal Length (y-axis) (mm)	1000							
Measured Length (y-axis)(µm	994.6	996.5	1001.4	1005.1	993.9	996.4	1004.1	1004.2
Deviation-y axis (µm)	-5.4	-3.5	1.4	5.1	-6.1	-3.6	4.1	4.2
Overall absolute deviation (µm)	6.0	3.8	2.3	6.0	6.8	5.5	4.8	7.4
Average Measured Length (µm)	1000.4				1001.2			
Average Measured Length from the two samples (µm)	1000.8							

6. Conclusions

This paper presents three generic integration tools for improving the system-level performance of reconfigurable laser micro-machining (LMM) platforms. The tools offer sufficient flexibility, robustness and operability to address important system-level issues in LMM and create the necessary pre-requisites for improving machining accuracy, repeatability and reproducibility (ARR) of LMM platforms. In particular, the research reports the design and implementation of modular workpiece holding device, automated workpiece setting up routine and automated strategy for multi-axis LMM machining with rotary stages that have a significant influence on the machining capabilities of LMM platforms. The following conclusions can be made:

1. System-level integration issues in LMM systems have been identified that limit their manufacturing capabilities and are important factors affecting their machining performance and also their broader use in various application areas.

2. Existing LMM systems can provide extensive manufacturing capabilities but their available system-level integration tools are not generic and far from what should be expected in machine tools for realising complex machining operations. Especially, the system-level component technologies that were identified as critical for improving the reliability, robustness and interoperability of LMM platforms and also to achieve the necessary machining ARR for their broader use are: modular workpiece holding device, automated workpiece setting up tools and automated multi-axis machining strategies.

3. The modular workpiece holding device allows different LMM configurations to be realised, e.g. the machining of complex prismatic and axis-symmetric parts, while delivering positional ARR better than +/- 1 μm, respectively. The design is based on the use of standardised commercially available components that can be used for manual or automated positioning of

the parts on LMM platforms. Furthermore, the modular design facilitates the integration of LMM systems into hybrid manufacturing platforms.

4. The developed automated strategy for multi-axis LMM employing rotary stages allows machining operations to be carried out with ARR better than +/- 6.5 μm, respectively.
5. The proposed automated workpiece setting up routine can be applied for LMM of complex free-from parts without the use of alignment marks. The routine is fully automated while delivering alignment ARR better than +/- 4 μm, respectively, by employing the proposed workpiece holding device and an FV probe. Due to the low resolution required to execute the setting up routine, a very good balance between its ARR and the time necessary to complete it can be achieved. It should be noted that the same alignment routine can be used if a FV probe is integrated in the LMM platforms and in this way the uncertainty associated with the routine can be reduced but in expense of the LMM platforms' throughput. In addition, in-line inspection routines similar to the workpiece's setting up one can be developed for implementing rest-volume machining strategies on LMM platforms and also for generating "customized" toolpaths for adaptive machining.

Acknowledgements

The research reported in this paper was supported by the FP7 NMP programme "High Performance Production Line for Small Series Metal Parts" (HYPROLINE), the INTERREG IVB NEW programme "ECO-efficient LASER technology for FACTories of the future (ECO-LASERFACT) and a project funded by Korean Government on "Laser-Based Modules for Functional Surface Texturing".

References:

1. European Comission. Factories of the Future: Multi‐Annual Roadmap for the Contractual PPP under HORIZON 2020. Luxembourg: Publications Office of the European Union 2013. ISBN 978-92-79-31238-0.
2. Stieglitz T. Manufacturing, assembling and packaging of miniaturized neural implants. Microsystem Technologies 2010; 16:723–734.
3. Lu J-Q. 3-D Hyperintegration and Packaging Technologies for Micro-Nano Systems. Proceedings of the IEEE 2009; 97: 18-30.
4. Dubey AK, Yadava V. Laser beam machining—A review. International Journal of Machine Tools and Manufacture 2008; 48:609–628.
5. Penchev P, et al. Novel manufacturing platform for scale up production of miniaturized components. In: International Workshop on Microfactories, Honolulu, 5-8 October 2014, pp.231-238.
6. Cheng J et.al. A review of ultrafast laser materials micromachining. Optics & Laser Technology 2013; 46: 88–102.
7. Chiu C-C and Lee Y-C. Fabricating of aspheric micro-lens array by excimer laser micromachining. Optics and Lasers in Engineering 2011; 49: 1232–1237.
8. Muhammad N. Laser micromachining of coronary stents for medical applications. PhD Thesis, University of Manchester, UK, 2012.
9. Huff MA and Ozgur M. Variable capacitor tuned using laser micromachining. Patent US 9019686 B2, USA, 2015.
10. Deng S, Penchev P and et al. Laser directed writing of flat lenses on buckypaper. Nanoscale. Accepted: 11th June 2015.
11. Vella PC, Dimov SS, Brousseau E and Whiteside BR. A new process chain for producing bulk metallic glass replication masters with micro- and nano-scale features. Int J Adv Manuf Technol 2015; 76:523–543.
12. Chu WS and et al. Hybrid Manufacturing in Micro/Nano Scale: A Review. Int. J.Precis. Eng. Manuf.-Green Tech. 2014; 1: 75-92.
13. Schubert A, Gros S, Schulz B and Eckert U. Sequential combination of micro-milling and laser structuring for manufacturing of complex micro-fluidic structures. Physics Procedia 2011; 12: 221-229.
14. Dimov S, Brousseau E, Minev R, et al. Micro- and nano- manufacturing: challenges and opportunities. Proc IMechE Part C: J Mech Eng Sci 2012; 226: 3–15.
15. Minev R, Vella P, Brousseau E, Dimov S, Minev E and Matthews C. Methodology for Capability Maturity Assessment of MNT chains. In: 4M conference on multi-material micro manufacture (ed B Fillon, C Khan-Malek and S Dimov), Bourg en Bresses and Oyonnax, 17-19 November 2010, pp. 249-253. Signpore: Research Publishing Services.
16. Kim K, Yoon K, Suh J and Lee J. Laser Scanner Stage On-The-Fly Method for ultrafast and wide Area Fabrication. Physics Procedia 2011; 12: 452–458.
17. Aerotech. Integrated automation solutions report: advanced control – Position Synchronized Output (PSO), 2013, http://www.aerotech.com/media/272125/ca0213b_controls_brochure_proof.pdfAerotech. Integrated Automation Solutions Report, 2013.
18. Penchev P, Dimov S, Bhaduri D, Soo SL and Crickboom B. Generic software tool for counteracting the dynamics effects of optical beam delivery systems. Proceedings of the Institution of Mechanical Engineers, Part B: Journal of Engineering Manufacture 2015 (published online)

19. Mirtchev T, Weeks R and Minko S. Optimizing the feedback control of Galvo scanners for laser manufacturing systems. In: Proceedings of SPIE: photonics north, 22 September 2010, 77500(T1-T7). Niagara Falls, Canada: SPIE.
20. Buls S, Craeghs T, Kempen K, et al. The influence of a dynamically optimized galvano based scanner on the total scan time of SLM parts. Report, University of Leuven,Belgium, August 2013.
21. Popov KB, Petkov PV, Layer based micro-machining: new approach for tool-path generation. CIRP Journal of Manufacturing Science and Technology 2011; 4: 370-375.
22. Pini S, Groppetti R and Senin N. Natural language manual programming for pulsed fiber laser micromachining. Int J Adv Manuf Technol 2013; 69:1451–1460.
23. Mutapcic E, Iovenitti P and Hayes JP. A prototyping and microfabrication CAD/CAM tool for the excimer laser micromachining process. Int J Adv Manuf Technol 2006; 30: 1076–1083.
24. Amplitude Systemes, Satsuma HP3 datasheet, 2015, http://www.amplitude-systemes.com/client/document/satsuma_3.pdf
25. Coffey V. Ultrafast and ultrashort: Some recent advances in pulsed lasers. Optics and Photonic News, May 2014, pp. 30-35, http://www.osa-opn.org/opn/media/Images/PDF/2014/0514/28-35_PulsedLasers2.pdf?ext=.pdf
26. Arnold C. Ultra-high speed variable focus elements for advance beam delivery. Industrial Laser Applications Symposium, 17-18 March 2015, Kenilworth, UK, http://www.ailu.org.uk/assets/document/presentations/15fmmargu17/88.pdf
27. Breit M, Muenzer H. Galvanometer Scanners with Digital PositionSensors Meet Industry's Toughest Challenges. Lasersystems Europe Whitepaper, Feb. 2015, Europa Science Ltd, http://www.scanlab.de/en/-/news_events/press/2015_02-LASERSYSTEMS_EUROPE#6713287
28. Aerotech. ADRS Series Stage User's Manual P/N: EDS108 (Revision 1.02.00), 2011.
29. Daemi B. Image analysis for precision metrology: Verification of micro-machining systems and aerodynamic surfaces. PhD Thesis, KTH Royal Institute of Technology, Sweden, 2014.
30. BS EN 60825-1:1994. Safety of laser products: Equipment classification, requirements and user's guide.
31. Bhaduri D, Penchev P, Dimov S, Soo SL. On comparative evaluation of accuracy, repeatability and reproducibility of laser micromachining systems. In: 4M/ICOMM (ed M Annoni, I Fassi, G Wiens and S Dimov), Milan, Italy, 31 March-2 April 2015, pp. 597-600. Singapore: Research Publishing Services.
32. Industrial laser solutions for manufacturing. Advanced laser processing systems magazine article, 2010, http://www.industrial-lasers.com/articles/2010/04/advanced-laser_processing.html
33. DMG MORI SEIKI Deutschland GmbH, Design offensive for demanding surface textures in injection moulds, Report, 2015, http://en.dmgmori.com/blob/120168/024215016ecb8aa18301858f9c5f4e09/pl0uk14-lasertec-shape-series-pdf-data.pdf
34. AgieCharmilles, Laser Texturing Solutions, Report, 2013, http://www.gfms.com/content/dam/gfac/proddb/Laser/Laser_EN.pdf
35. Pham DT, Dimov SS and Petkov PV. Laser milling of ceramic components. International Journal of Machine Tools and Manufacture 2007; 47:618–626.
36. Petkov PV. Development and Implementation of Technology for Laser Micro Structuring of Roller. In: 4M conference on multi-material micro manufacture (ed B Fillon, C Khan-Malek and S Dimov), Bourg en Bresses and Oyonnax, 17-19 November 2010, pp. 249-253. Signpore: Research Publishing Services.

37. Dausinger F and Sommer S. Ultrafast laser processing: From Micro to Nano scale Industrial applications. In: Sugioka K and Cheng Y (eds) Ultrafast Laser Processing. USA: Taylor & Francis Group, 2013, pp.569-586.
38. System 3R. Reference systems for electrode manufacturing & EDMing report, 2012, http://www.system3r.ch/PDF/T-2389-e_edm.pdf
39. Aerotech. PRO165LM Series Stage User's Manual P/N: EDS142 (Revision 1.06.00), 2010.
40. Schille J and etc.all. Micro Processing of Metals Using a High Repetition Rate Femtosecond Laser: from Laser Process Parameter Study to Machining Examples. In: International Congress on Applications of Lasers & Electro-Optics, Orlando, 23-27 October 2011, pp. 773-782.
41. PD ISO/TR 16907:2015. Machine tools — Numerical compensation of geometric errors.
42. Bohez ELJ. Five-axis milling machine tool kinematic chain design and analysis. International Journal of Machine Tools and Manufacture 2002; 42: 505-520.
43. Huang N, Jin Y, Bi Q, Wang Y. Integrated post-processor for 5-axis machine tools with geometric errors compensation. International Journal of Machine Tools and Manufacture 2015; 94: 65-73.
44. Shmitt R, Mallmann G. Process monitoring in laser micromachining.Manufacturing Technology 2013, 57-59
45. Bello SM. New results from the examination of cut-marks using three-dimensional imaging, Developments In Quaternary Science 2011; 14: 249-262.
46. Alicona. Alicona Focus Variation magazine: Form and roughness in one system. Edition 5, 2015
47. Vijayaraghavan A,Hoover AM, Hartnett J, Dornfeld DA. Improving endmilling surface finish by workpiece rotation and adaptive toolpath spacing. International Journal of Machine Tools and Manufacture 2009; 49: 89-98.
48. Renishaw, Adaptive machining, 2012, http://resources.renishaw.com/en/details/ap210-productive-process-pattern-adaptive-machining--39412
49. Alicona Imaging. IF-Measure Suite manual. Alicona measuring suite manual Version 4.1, 2013.
50. Schwenke H, Knapp W, Haitjema H, Weckenmann A, Schmitt R, Delbressine F. Geometric error measurement and compensation of machines—An update. CIRP Annals - Manufacturing Technology 2008; 57: 660–675.
51. Aerotech. Optec's multi-wavelength ultrafast laser micromachining workstation features novel turret optics design using Aerotech micro positioning and motion controls. Aerotech Articles on Laser processing and micromachining, 2013, Accessed on: 22.10.2015, http://motioncontrol.aerotech.com/2013/03/12/micromachining-novel-turret-optics/